Plant Cell Advance Publication. Published on February 21, 2017, doi:10.1105/tpc.16.00791

RESEARCH ARTICLE

RIMA-dependent nuclear accumulation of IYO triggers auxin-irreversible cell differentiation in Arabidopsis

Alfonso Muñoz[a], Silvina Mangano[a,1,4], Mary Paz González-García[a,4], Ramón Contreras[a], Michael Sauer[a,2], Bert De Rybel[b,3], Dolf Weijers[b], José Juan Sánchez-Serrano[a], Maite Sanmartín[a,5] and Enrique Rojo[a,5]

[a]Centro Nacional de Biotecnología-CSIC, Cantoblanco, E-28049 Madrid, Spain.
[b]Wageningen University, Laboratory of Biochemistry, Dreijenlaan 3, 6703 HA Wageningen.
[1]Current address: Fundación Instituto Leloir, Buenos Aires, Argentina, C1405BWE.
[2]Current address: Department of Plant Physiology, University of Potsdam, 14476 Potsdam, Germany.
[3]Current address: Department of Plant Systems Biology, VIB, B-9052 Ghent, Belgium and Department of Plant Biotechnology and Bioinformatics, Gent University, B-9052 Ghent, Belgium.
[4]These authors contributed equally to this work
[5]Corresponding Authors: msanmart@cnb.csic.es or erojo@cnb.csic.es; fax: 34915854506

Short title: RIMA/IYO nuclear differentiation switch

One-sentence summary: The Arabidopsis RPAP2/RTR1 homologue RIMA interacts with IYO and mediates its nuclear accumulation to activate cell differentiation that cannot be reversed by auxins.

The authors responsible for distribution of materials integral to the findings presented in this article in accordance with the policy described in the Instructions for Authors (www.plantcell.org) are: Enrique Rojo (erojo@cnb.csic.es) and Maite Sanmartín (msanmart@cnb.csic.es).

ABSTRACT

The transcriptional regulator MINIYO (IYO) is essential and rate-limiting for initiating cell differentiation in *Arabidopsis thaliana*. Moreover, IYO moves from the cytosol into the nucleus in cells at the meristem periphery, possibly triggering their differentiation. However, the genetic mechanisms controlling IYO nuclear accumulation were unknown and the evidence that increased nuclear IYO levels trigger differentiation remained correlative. Searching for IYO interactors, we have identified RPAP2 IYO Mate (RIMA), a homologue of yeast and human proteins linked to nuclear import of selective cargo. Knockdown of *RIMA* causes delayed onset of cell differentiation, phenocopying the effects of *IYO* knock down at the transcriptomic and developmental levels. Moreover, differentiation is completely blocked when *IYO* and *RIMA* activities are simultaneously reduced and is synergistically accelerated when *IYO* and *RIMA* are concurrently overexpressed, confirming their functional interaction. Indeed, *RIMA* knockdown reduces the nuclear levels of IYO and prevents its pro-differentiation activity, supporting the conclusion that RIMA-dependent nuclear IYO accumulation triggers cell differentiation in Arabidopsis. Importantly, by analysing the effect of the IYO/RIMA pathway on xylem pole pericycle cells, we provide compelling evidence reinforcing the view that the capacity for *de novo* organogenesis and regeneration from mature plant tissues can reside in stem cell reservoirs.

51

INTRODUCTION

Stem cell progeny may retain pluripotency to renew the stem cell pool or undergo differentiation to acquire specialized functions. This cell fate decision is under strict genetic control to assure proper development of the organism, but the circuitry controlling and executing this choice is still largely unknown (Benfey, 2016). Moreover, in certain organisms this decision may be revoked and differentiated cells can return into a stem cell state (Sugimoto et al., 2011; Sanchez Alvarado and Yamanaka, 2014). Unravelling if and how cells may be reprogrammed into pluripotency is key for understanding processes such as regeneration, wound healing and somatic cloning. Plants in particular have a high capacity for regenerating organs and even the whole organism (Sugimoto et al., 2011; Liu et al., 2014). Moreover, callus cultures of pluripotent stem cells are easily obtained from many plant species by incubating mature tissues in auxin-rich media (Atta et al., 2009; Sugimoto et al., 2010; Ikeuchi et al., 2013). These findings have led to the widely-held hypothesis that plant cells can readily dedifferentiate into pluripotency (Iwase et al., 2011b; Chupeau et al., 2013; Ikeuchi et al., 2013; Ikeuchi et al., 2015; Sugiyama, 2015). However, plants retain reservoirs of undifferentiated cells in adult tissues, such as the stem cell populations in apical meristems that generate post-embryonically most of the organs of the plant (Scheres, 2007; Wolters and Jurgens, 2009). Thus, stem cells present in adult tissues could be the source for callus formation and for organ regeneration, bypassing the need for a dedifferentiation step. Indeed, it has been now convincingly shown that auxin-induced callus cultures derive from xylem pole pericycle and pericycle-like cambium cells (Che et al., 2007; Atta et al., 2009; Sugimoto et al., 2010; Liu et al., 2014), which have meristematic characteristics (Beeckman et al., 2001; Atta et al., 2009; Liu et al., 2014). Moreover, in a root tip regeneration assay, the competence for regeneration was mapped to the root apical meristem cells (Sena et al., 2009). These results suggest that pre-existing stem cells are the source for auxin-induced callus formation and possibly for organ regeneration in plants, but definitive proof of this is lacking.

Cell fate conversions are in essence a matter of altering genome expression. Indeed, the conversion from pluripotency into differentiation implies large changes in genome transcription, to activate cell lineage developmental programs and turn off stem cell self-renewal programs (Sablowski, 2011; Young, 2011). In metazoans, the implementation of these mutually exclusive transcriptional states is in large part dependent on regulation at the elongation phase of transcription (Guenther et al., 2007; Stock et al., 2007; Brookes et al., 2012). In plants, factors regulating transcriptional elongation also play key roles in development (Sanmartin et al., 2012; Van Lijsebettens and Grasser, 2014). In particular, the *Arabidopsis thaliana MINIYO* (*IYO*) gene encodes an RNA polymerase II (Pol II)-interacting factor that sustains transcriptional elongation in developing organs and is essential for initiating cell differentiation throughout the plant. *IYO* is rate limiting for cell differentiation and accumulates in the nucleus with timing that coincides with the onset of cell differentiation, suggesting that increased nuclear IYO levels may trigger this cell fate transition (Sanmartin et al., 2011). However, the genetic mechanisms that determine the subcellular localization of IYO have remained unknown and we have lacked direct evidence that nuclear accumulation of IYO is required for its pro-differentiation activity.

Proteomic studies aimed at characterizing the components of the human transcriptional machinery uncovered a set of four RNA Polymerase II Associated Proteins (RPAPs) that are conserved in all eukaryotic kingdoms (Jeronimo et al., 2007). RPAPs form an interaction network that is tightly connected to the Pol II complex in the nuclear compartment (Jeronimo et al., 2007; Boulon et al., 2010; Forget et al., 2010). RPAP1, the human homologue of Arabidopsis IYO, forms part of the functionally active Pol II complex and is thought to directly regulate transcription (Jeronimo et al., 2004). Human RPAP2 and RPAP4/GPN1, and their yeast counterparts RTR1 and NPA3, have been ascribed diverse functions in assembly, nuclear import and regulation of Pol II activity (Forget et al., 2010; Calera et al., 2011; Carre and Shiekhattar, 2011; Staresincic et al., 2011; Egloff et al., 2012; Forget et al., 2013; Minaker et al., 2013; Wani et al., 2014; Gomez-Navarro and Estruch, 2015; Niesser et al., 2016). However, very little is known in

yeast and animals about the biological processes in which these RPAP proteins are involved. In yeast, the homologues of *RPAP1*, *RPAP2* and *RPAP4* are either essential for viability (Giaever et al., 2002) or cause severe growth defects when mutated (Gibney et al., 2008), supporting the conclusion that they play fundamental, although yet uncharacterized roles in the physiology of these organisms. In animals, siRNA knockdown of *RPAP2* and *RPAP4* in immortalized cell lines interferes with nuclear import and activity of Pol II (Forget et al., 2010; Calera et al., 2011; Carre and Shiekhattar, 2011; Egloff et al., 2012; Forget et al., 2013; Wani et al., 2014), but the physiological *in vivo* roles of these genes remain unexplored..

Here, in searching for IYO interactors, we identified the RPAP2 homologue RIMA and the RPAP4 homologues GPN1 and GPN2. Arabidopsis T-DNA insertional mutants in *GPN1* and *GPN2* arrest at the octant/16-cell stage of embryogenesis (Lahmy et al., 2007), which hampers genetic characterization of their developmental roles. Accordingly, we focused our functional analysis on *RIMA*, which was unexplored to date. The results we present strongly support the conclusion that RIMA is an essential partner of IYO in activating cell differentiation and suggest that this is a process that cannot be reversed.

RESULTS

IYO interactors are conserved from plants to humans

Identification by mass-spectrometry of proteins co-immunopurifying with a functional IYO-GFP protein (Supplemental Table 1) and confirmation by bimolecular fluorescence complementation (BiFC) and pull down assays (Figure 1A and Sanmartin et al., 2011) revealed that IYO interacts with the Pol II subunits RPB2, RPB3, RPB10 and RPB11, and with the RPAP4 homologues GPN1 and GPN2. Interestingly, the human IYO homologue RPAP1 has also been found in a complex with RPB2, RPB3, RPB10, RPB11, RPAP4/GPN1 and GPN2, as well as with an additional RPAP protein, RPAP2 (Boulon et al., 2010). The Arabidopsis genome contains a homologue of RPAP2 encoded by the *RPAP2 IYO MATE* (*RIMA*/At5g26760) gene, which was not identified among the proteins co-purifying with IYO-GFP. However, in these experiments IYO-GFP was constitutively expressed under the 35S promoter, which could dilute out the fraction interacting with RIMA, which has a restricted domain of expression (see below), and prevent detection of the interaction. Indeed, we observed BiFC interaction between IYO and RIMA when we co-expressed both proteins in *Nicotiana benthamiana* leaves (Figure 1B). The BiFC interaction with IYO was abolished by point mutations that disrupt the RIMA zinc finger domain (Figure 1C), which is conserved in RIMA homologues from plants, yeast and mammals (Supplemental Figure 1) and has been proved essential for the *in vivo* activity of yeast RTR1 (Gibney et al., 2008). To confirm the interaction between IYO and RIMA, we raised specific antibodies against RIMA (Supplemental Figure 2). We observed co-purification of HA-tagged IYO when we immunopurified the endogenous RIMA (Figure 1D), indicating that the two proteins interact *in vivo*. Together, these results show that the IYO/RPAP1 interactome is conserved from plants to animals and includes a Pol II subcomplex, GPN GTPases and RIMA.

RIMA is expressed in meristems where it shuttles through the cytosol and the nucleus

To determine the expression profile of *RIMA*, we analyzed plants expressing GUS under the control of the *RIMA* promoter (*ProRIMA:GUS*). In the aerial part of the plant, *ProRIMA:GUS* expression was highest in the shoot apical meristem (SAM), in leaf and flower primordia, in ovules and in developing embryos (Figure 2A). In the root, strong *ProRIMA:GUS* signal was observed in the root apical meristem (RAM), in the transition zone and in lateral root primordia (Figure 2B). This promoter activity domain largely overlaps with that of the *IYO* promoter (Sanmartin et al., 2011), and is in agreement with high degree of co-expression between the *IYO* and *RIMA* transcripts (Pearson correlation coefficient of 0.62) found using the ACT tool (Jen et al., 2006). To characterize the subcellular distribution of RIMA, we used as a proxy a functional *ProRIMA:RIMA-GFP* construct that complements all *rima* mutant phenotypes (see below). In roots of *ProRIMA:RIMA-GFP rima-1* plants, strong GFP fluorescence was observed in the RAM, in the transition zone and in lateral root primordia (Figure 2C), matching the activity profile of the *ProRIMA:GUS* plants. The fluorescence was primarily cytosolic, but it was also detectable in the nucleus (Figure 2D-E). Similarly, fluorescence was largely cytosolic in *N. benthamiana* leaves transiently transformed with *Pro35S:RIMA-GFP* (Figure 2F). The yeast and human homologues RTR1 and RPAP2 are also localized at steady state primarily in the cytosol, but they redistribute to the nucleus upon inhibition of the XPO1 nuclear export receptor with Leptomycin B (LMB) (Gibney et al., 2008; Forget et al., 2013), which also blocks the Arabidopsis XPO1 receptor (Haasen et al., 1999). Treatment with LMB resulted in higher nuclear levels of RIMA-GFP (Figure 2F-G), confirming that RIMA shuttles between the cytosol and the nucleus in plants.

RIMA activity is required for cell differentiation

To analyze the *in vivo* function of RIMA, we characterized two T-DNA insertional lines from the SALK collection, *rima-1* (SALK_012339) and *rima-2* (SALK_11576). Homozygous plants for the *rima-1* allele, containing a T-DNA insertion in the first

exon of the gene, could not be recovered. In siliques from *rima-1/RIMA* heterozygous plants, the growth of 26% of the seeds (n=472) was abnormal and eventually ceased. Analysis of the arrested seeds showed that *rima-1* embryos develop aberrantly, retaining a globular morphology lacking any discernible cotyledon, hypocotyl or root structures, and eventually aborting at mature stage (Figure 3A). Notably, these defects in embryonic organogenesis are similar to those observed in strong *iyo* alleles (Sanmartin et al., 2011). By contrast, plants homozygous for the *rima-2* allele, which contains a T-DNA insertion in the third intron of the gene, were viable and fertile but developed abnormally, displaying similar alterations as the *iyo-1* knockdown mutant (Sanmartin et al., 2011). The *rima-2* plants showed delayed leaf emergence, altered phyllotaxis and perturbed leaf morphology (Figure 3B). Moreover, the SAM was enlarged, splitting into several meristems, and generating highly fasciated stems (Figure 3C-D). Splitting of flower meristems was also observed in *rima-2* plants, which gave rise to compound flowers and siliques (Figure 3D). These alterations suggest that *RIMA* is required for proper cell differentiation and organogenesis in the SAM. Likewise, differentiation was delayed and defective in the protoderm of *rima-2* cotyledons (Figure 3E), which are organs of embryonic origin. At a stage when the wild-type (Wt) cotyledon epidermis was fully differentiated, the *rima-2* epidermis still retained small protoderm-like cells expressing the *ProTMM:TMM-GFP* stem cell marker. We also observed developmental alterations indicative of defective differentiation in the *rima-2* RAM. In the proximal side, ectopic periclinal divisions of ground tissue cells broadened the meristem (Figure 3F), while in the distal side, differentiating columella cells abnormally retained expression of a stem cell marker (Figure 3G). These developmental alterations are shared with the *iyo-1* mutant (Sanmartin et al., 2011) and demonstrate that *RIMA* is required for proper cell differentiation throughout the plant.

Expression analysis revealed that *rima-2* plants accumulate much reduced levels of the full-length transcript and the corresponding protein, besides accumulating a shorter *RIMA* transcript encoding a truncated protein (Figure 3H and Supplemental Figure 2A). This suggests that the intron containing the T-DNA

in *rima-2* is spliced out with low efficiency, causing an acute reduction in the expression of the full-length protein. The *rima-2* allele was fully recessive and developmental perturbations were worsened in trans-heterozygous *rima-1/rima-2* plants, which showed further delay in leaf emergence, larger meristems and increased shoot fasciation relative to the *rima-2* homozygous mutant (Figure 3I). Moreover, all phenotypes of *rima-1* and *rima-2* mutants were complemented by transformation with a genomic *RIMA* sequence, which demonstrated that they were due to the disruption of the *RIMA* gene. From these results, we conclude that *rima-1* is a null allele that provokes a complete block in organogenesis and is embryo lethal, while *rima-2* is a knockdown allele with reduced expression of full-length *RIMA* that causes defective cell and organ differentiation throughout an otherwise viable plant. RIMA fused to GFP under the control of the *RIMA* promoter (*ProRIMA:RIMA-GFP*) also complemented the *rima* mutants (Figure 3J, note rescue of plant death and of the irregular pattern of leaf emergence in *ProRIMA:RIMA-GFP rima-1* plants), indicating that the *ProRIMA:RIMA-GFP* construct fully recapitulates the expression and activity of the endogenous *RIMA* gene. Transformation with *Pro35S:RIMA-GFP* also rescued *rima-1* lethality (Figure 3J), but a zinc-finger mutant version (*Pro35S:RIMA*$_{C94A/C98A}$*-GFP*) failed to complement it, indicating that this domain is essential for RIMA function. Notably, complementation in the *Pro35S:RIMA-GFP rima-1* plants was partial, and the plants phenocopied the adult phenotype of *rima-2* knock down mutants, including delayed leaf emergence (Figure 3J). This partial complementation corresponded with lower expression of the transgene than in the fully complemented *ProRIMA:RIMA-GFP rima-1* lines (Figure 3J). Interestingly, twin embryos developed frequently in *Pro35S:RIMA-GFP rima-1* seeds (Figure 3K), implying that when *RIMA* activity is insufficient, ectopic totipotent stem cells are retained. Together, these phenotypes indicate that *RIMA* is required for initiating cell differentiation throughout the plant.

The *iyo-1* and *rima-2* mutants have matching transcriptomic fingerprints

Qualitatively, the developmental phenotypes of *rima* and *iyo* mutants are very similar (Sanmartin et al., 2011), consistent with *RIMA* and *IYO* regulating common downstream processes. To gain a quantitative measure of their phenotypic identity, we compared the transcriptome alterations in inflorescences (consisting of the SAM and developing flowers) of the *iyo-1* and *rima-2* mutants relative to those of Wt plants. This analysis revealed a striking similarity between the mutants. The overlap between the sets of genes that were most strongly down-regulated (top 400 genes by fold-change) in each mutant to Wt comparison (genes that require *IYO* and *RIMA* for full expression) was 31-fold higher than expected at random (p-value=1.57e-295, hypergeometric test, Figure 4A) and 12-fold higher (p-value=3.45e-66, hypergeometric test) for the genes most strongly up-regulated in both mutants. In all, 372 out of the 400 most down-regulated genes in *iyo-1* were also down-regulated in *rima-2* (Figure 4B) and 352 out of the 400 most up-regulated genes in *iyo-1* were up-regulated in *rima-2*. Geneset enrichment analysis (GSEA) showed that pathways related to morphogenesis and flower organogenesis were enriched among the down-regulated genes in inflorescences from both mutants (Figure 4C). These common down-regulated genes included all floral organ identity genes (Supplemental Table 2), which act as master regulators for differentiation and organogenesis in inflorescence meristems (Sablowski, 2015). These results indicate that IYO and RIMA are required for activating common genetic programs related with organogenesis.

IYO and _RIMA_ cooperate genetically to activate differentiation

The remarkable degree of gene co-regulation in the mutants provides robust quantitative support for the hypothesis that *IYO* and *RIMA* function in the same developmental pathway. To further explore this hypothesis, we tested for their genetic interaction. We first analyzed the effect of a simultaneous reduction in the activity of both genes by crossing the *iyo-1* and *rima-2* knockdown mutants. The *iyo-1 rima-2* double mutant seedlings failed to develop proper organs, and eventually developed into a friable callus-like mass of cells that could be propagated *in vitro* without external addition of hormones (Figure 5A-B). The

majority of the cells in those calli had either 2C or 4C DNA content (Figure 5C), demonstrating that they consisted mainly of mitotically active cells. The synergistic inhibition of cell differentiation when combining the *iyo-1* and *rima-2* mutations is consistent with *RIMA* and *IYO* cooperating in a function that is essential for cells to differentiate. To confirm this genetic interaction, we analyzed the effect of concurrent overexpression of *IYO* and *RIMA*. We reported previously that overexpression of HA-tagged IYO under the constitutive 35S promoter (*Pro35S:IYO-HA* lines) causes premature onset of cell differentiation and eventually, meristem termination (Sanmartin et al., 2011). Although expression of *RIMA* tagged with HA, Flag or GFP under the same 35S promoter did not produce any evident developmental phenotype on its own, when combined with the *Pro35S:IYO-HA* transgene, a synergistic acceleration of SAM termination was observed (Figure 5D), indicating that *IYO* and *RIMA* cooperatively activate cell differentiation.

RIMA mediates IYO nuclear accumulation to activate cell differentiation

Considering that RIMA and IYO interact physically, we presumed that their genetic cooperation reflected cross activation at the protein level. Based on the reported function of RPAP2 and RTR1 in nuclear import in mammals and yeast, we hypothesized that RIMA could activate IYO by mediating its nuclear accumulation. Thus, we compared the localization of *ProIYO:IYO-GFP* in Wt and *rima-2* mutant plants. As previously reported (Sanmartin et al., 2011), *ProIYO:IYO-GFP* fluorescence in Wt roots showed a diffuse cytosolic distribution in cells at the meristem core, but concentrated in the nucleus of cells at the meristem periphery (Figure 6A). In *rima-2* roots there was a strong reduction in IYO-GFP nuclear accumulation across the root, which was coupled to increased cytosolic levels (Figure 6A). Moreover, nuclear IYO-GFP accumulation was restored when *rima-2* plants were incubated in the presence of LMB, demonstrating that reduced RIMA activity impairs nuclear targeting of IYO-GFP and not its expression. This role in transport of IYO into the nucleus is consistent with the steady-state localization of RIMA in the cytosol and its redistribution to the nucleus when irreversibly linked to

IYO in the BiFC complex (Figure 1B). Moreover, co-expression with IYO-HA in *N. benthamiana* leaves increased the nuclear RIMA-GFP levels relative to plants expressing RIMA-GFP alone (Figure 6B), consistent with RIMA escorting IYO during transport into the nucleus. We reasoned from these results that if nuclear accumulation were required for IYO pro-differentiation function, then the *rima-2* mutation should be epistatic on *IYO* activity. To check this, we introgressed *Pro35S:IYO-HA* into the *rima-2* mutant background. The *rima-2* mutation suppressed meristem termination caused by *IYO-HA* overexpression (Figure 6C, note the indeterminate SAM growth of *Pro35S:IYO-HA rima-2* plants), indicating that IYO requires RIMA to activate differentiation. To exclude the possibility that the suppression of the phenotype was due to silencing of the *IYO-HA* transgene, we analyzed its expression. The levels of IYO-HA were actually increased in the *rima-2* background (Figure 6C), demonstrating that *RIMA* activity is required for *IYO* overexpression to induce premature differentiation and suggesting that a compensatory mechanism increases IYO protein accumulation when *RIMA* activity is compromised. All together, these genetic analyses support the conclusion that RIMA mediates nuclear IYO accumulation to activate cell differentiation.

Forced differentiation of xylem pole pericycle cells blocks lateral root formation and callus growth.

It is still disputed whether lateral root formation, callus growth and subsequent plant regeneration involves a process of dedifferentiation or rather results from the expansion of undifferentiated cells present in the starting tissue (Atta et al., 2009; Sugimoto et al., 2010; Iwase et al., 2011b; Iwase et al., 2011a; Chupeau et al., 2013; Ikeuchi et al., 2013; Liu et al., 2014; Sanchez Alvarado and Yamanaka, 2014; Sugiyama, 2015). Lateral roots and calli derive from xylem pole pericycle cells and pericycle-like cambium cells (Dubrovsky et al., 2000; Beeckman et al., 2001; Che et al., 2007; Atta et al., 2009; Sugimoto et al., 2010; Liu et al., 2014). Although their actual differentiation status remains unknown, it has been shown that they retain certain meristematic properties (Beeckman et al., 2001; Atta et al., 2009; Liu et al., 2014). In this regard, a hallmark of undifferentiated cells in apical

meristems is the exclusion of IYO-GFP from the nucleus (Sanmartin et al., 2011). To determine if this is also the case in xylem pole pericycle cells, we analyzed the localization of IYO-GFP in the mature zone of the root, using as control the nuclear marker RPB10-GFP expressed under the same 35S promoter. Both RPB10-GFP and IYO-GFP were found to accumulate in the nuclei of cells from the epidermis, the cortex, the endodermis and the vasculature. By contrast, only RPB10-GFP was detectable in the nucleus of xylem pole pericycle cells (Figure 7A and Supplemental Figure 3; *Pro35S:RPB10-GFP* roots: 4-6 GFP positive xylem pole pericycle nuclei per field of view; *Pro35S:IYO-GFP*: 0 GFP positive xylem pole pericycle nuclei per field). Incubation with auxins induces proliferation of xylem pole pericycle cells, which undergo periclinal divisions to form a multilayer tissue that eventually develops into a callus. RPB10-GFP labelled the nuclei of the auxin-induced multilayer xylem pole pericycle, but IYO-GFP was conspicuously absent from their nuclei (Figure 7B). Likewise, in the mature zone of the root *ProIYO:IYO-GFP* was expressed specifically in xylem pole pericycle cells, but it did not accumulate in the nucleus (Supplemental Figure 4). These results support that xylem pole pericycle cells specifically exclude IYO from the nucleus to remain undifferentiated, similarly to cells in apical meristems. It follows from this premise that increasing the expression of *IYO* and *RIMA* may cause their differentiation and possibly result in defects in lateral root formation and callus generation. In agreement with this, plants overexpressing *IYO* and *RIMA* rarely formed lateral root primordia, which ceased growth prior to or shortly after emergence, causing a "solitary root" phenotype (Figure 7C). Moreover, in contrast to the widespread proliferation of xylem pole pericycle cells that is induced in Wt roots incubated in auxin-rich media, overexpression of *IYO* caused more discrete foci of pericycle cell proliferation and reduced callus formation, and over expression of *IYO* and *RIMA* severely impaired xylem pole pericycle proliferation and callus formation (Figure 7D-E). These results indicate that auxin-treatment alone does not revert differentiation triggered by IYO and RIMA. Moreover, these findings support the emerging paradigm that pre-existing stem cells are necessary for auxin-induced callus formation and lateral root development in plants. However, we cannot

exclude that a step of dedifferentiation, blocked by overexpression of *IYO* and *RIMA*, may be involved in these processes.

DISCUSSION

Regulation of the IYO/RIMA cell differentiation switch

Our results identify RIMA as an essential partner of IYO for inducing cell differentiation in Arabidopsis. Although the two partners are co-regulated at the transcriptional level, there is evidence of differential post-translational regulation of their localization and activities. Whereas RIMA has a uniform and primarily cytosolic distribution across the root tip, IYO localization changes markedly from the meristem core to the periphery, where it accumulates in the nucleus coinciding with the onset of cell differentiation (Sanmartin et al., 2011). Furthermore, we did not observe any effect when RIMA was overexpressed on its own, while *IYO* overexpression activated premature differentiation. These data support the conclusion that RIMA activity is constitutive and sufficient for differentiation, whereas IYO activity is highly regulated and rate limiting for differentiation. In fact, RIMA becomes limiting for differentiation in the context of IYO overexpression, which is fully consistent with a role in mediating nuclear IYO accumulation. In agreement with a constitutive RIMA activity, RIMA knockdown causes lower levels of nuclear IYO accumulation both in meristematic cells, where IYO-GFP becomes totally excluded from the nucleus, and in transition cells, where only weak nuclear accumulation is observed. Constitutive activity of RIMA throughout the meristem may allow meristematic cells to rapidly enter differentiation, or, alternatively, it may reflect additional roles of RIMA in undifferentiated cells. The observation that RIMA-dependent nuclear IYO import is operative, albeit at low rate, in meristematic cells explains how *IYO* overexpression can induce their premature differentiation and why this is blocked when *RIMA* activity is knocked down. These data also suggest that RIMA is required but not responsible for generating the gradient of IYO nuclear accumulation. Conditional post-translational modifications of IYO or additional partners could differentially modulate the interaction of IYO with the

constitutively active RIMA to regulate the rate of import and generate the nuclear abundance gradient. Considering that GPN proteins are conserved partners of IYO and RIMA that have been implicated in nuclear import in yeast and humans (Forget et al., 2010; Calera et al., 2011; Carre and Shiekhattar, 2011; Staresincic et al., 2011), it will be worth exploring their role in RIMA-dependent IYO transport. Moreover, RPAP2 and RTR1 have been assigned nuclear functions independent of their roles in protein import. A number of reports suggest that RPAP2/RTR1 are responsible for dephosphorylating Pol II during transcriptional elongation (Mosley et al., 2009; Egloff et al., 2012; Hsu et al., 2014; Ni et al., 2014; Hunter et al., 2016), a striking link to IYO nuclear function. Although it has been questioned whether RTR1 had intrinsic phosphatase activity (Xiang et al., 2012), a recent structural analysis revealed a putative active site in RTR1 and identified several residues important for phosphatase activity (Irani et al., 2016). Those residues are conserved in RIMA, which accordingly may also have Pol II phosphatase activity. It is thus possible that IYO and RIMA maintain their cooperation after import into the nucleus to regulate Pol II transcriptional activity, an intriguing hypothesis to pursue.

Stem cell reservoirs for regeneration in plants

Although dedifferentiation is a widely-documented phenomenon in plants (Iwase et al., 2011b; Chupeau et al., 2013; Ikeuchi et al., 2013; Ikeuchi et al., 2015; Sugiyama, 2015), recent studies have questioned its general involvement in *de novo* organogenesis and regeneration (Sugimoto et al., 2011; Gaillochet and Lohmann, 2015). Detailed morphological analysis in Arabidopsis has shown that lateral roots and calli derive from root xylem pole pericycle cells or leaf pericycle-like cambium cells (Dubrovsky et al., 2000; Beeckman et al., 2001; Atta et al., 2009; Sugimoto et al., 2010; Liu et al., 2014). Moreover, callus formation in roots is severely impaired when xylem pole pericycle cells are ablated through specific expression of diphteria toxin chain A (Che et al., 2007), supporting the idea that they are the unique source for callus growth in roots. Although the actual differentiation status of xylem pole pericycle cells is unknown, they have meristematic characteristics that distinguish them from the surrounding cell layers

441 in the mature root: they retain diploidy, express cell-cycle genes, rapidly re-enter
442 mitosis to form lateral root primordia (Beeckman et al., 2001; Atta et al., 2009; Liu
443 et al., 2014) and exclude IYO from the nucleus (this work). By forcing differentiation
444 throughout the plant, we have now provided conclusive evidence suggesting that
445 xylem pole pericycle cells are indeed stem cells that need to remain
446 undifferentiated to generate lateral roots during normal development, and callus in
447 auxin-rich media. Thus, our results support the emerging view that stem cell
448 reservoirs present in the adult tissues can be the source for *de novo*
449 organogenesis, auxin-induced callus formation and subsequent regeneration in
450 plants (Gaillochet and Lohmann, 2015). This paradigm shift means that to
451 understand these processes we need to focus on studying how plants regulate the
452 fate of stem cell reservoirs in adult plant tissues. Auxins and cytokinins are likely to
453 play a key role in their regulation, given their central function in lateral root
454 development, callus formation and regeneration (Fukaki et al., 2007; Ikeuchi et al.,
455 2013; Perianez-Rodriguez et al., 2014; Su and Zhang, 2014). In addition, very-
456 long-chain fatty acids and, not surprisingly, tissue aging have recently been shown
457 to restrict regeneration potential in Arabidopsis (Zhang et al., 2015; Shang et al.,
458 2016). Moreover, several genes required for lateral root development and callus
459 formation, apart from *IYO* and *RIMA*, have been characterized: the cell cycle
460 regulator *KRP2* (Sanz et al., 2011; Cheng et al., 2015), the regulators of auxin
461 signalling genes *ARF7, ARF19* and *SLR1* (Fukaki et al., 2002; Okushima et al.,
462 2007; Fan et al., 2012; Shang et al., 2016), the transcription factors *LBD16,*
463 *LBD17, LBD18, LBD29* (Okushima et al., 2007; Lee et al., 2009; Fan et al., 2012)
464 and the plant-specific *ALF4* gene (DiDonato et al., 2004; Sugimoto et al., 2010). A
465 key challenge for the future will be to unravel how these genetic networks integrate
466 hormonal and metabolic signals to regulate the fate of stem cell reservoirs in adult
467 tissues during development and in response to environmental cues.
468
469 **METHODS**
470 **Plant Materials and Growth Conditions**

The T-DNA insertion lines in the Col-0 background *rima-1* (SALK_012339) and *rima-2* (SALK_11576) were obtained from the Arabidopsis Stock Center and genotyped using specific primers (Supplemental Table 3). The *iyo-1* mutant and the *ProSTM:GUS*, *ProTMM:TMM-GFP*, *J2341*, *Pro35S:RPB10-GFP*, *Pro35S:IYO-GFP, ProIYO:IYO-GFP* and *Pro35S:IYO-HA* lines used were previously described (Sanmartin et al., 2011). Plants were grown on soil in the greenhouse under natural light, supplemented with Osram HQL 400w sodium lamps when illuminance fell below 5000 lx, and a 16h light/8h dark cycle at a temperature range between 22ºC maximum/18ºC minimum. For *in vitro* culture, plants were grown at 22ºC under 6000 luxs of illuminance in a 16h light/8 h dark cycle.

Constructs

RIMA coding sequence, promoter and genomic DNA were PCR amplified using primers listed on Supplemental Table 3 and cloned into pDONR207 vector for Gateway recombination-based subcloning (Invitrogen). The following destination vectors were used: pGWB3 (for ProRIMA:GUS), pGWB4 (for ProRIMA:RIMA-GFP, and pGWB5 (for Pro35S:RIMA-GFP). For bimolecular fluorescence complementation, *RIMA*, *GPN* and *IYO* coding sequences were amplified with primers shown in Supplemental Table 3, cloned into pDONR207 vector for Gateway recombination-based cloning in pBIFP vectors and agroinfiltrated into leaves of *Nicotiana benthamiana* as described (Sanmartin et al., 2011).

Chemicals and treatments

For in vitro culture, plants were grown in medium containing Murashige and Skoog salts and 1% sucrose, with (solid MS) or without (liquid MS) 0.7% agar. For Leptomycin B treatments, agroinfiltrated *N. benthamiana* leaves or *Arabidopsis thaliana* seedlings were incubated in liquid MS containing 0.9 μM Leptomycin B before imaging by confocal microscopy. For callus induction assays, sections from the mature zone of roots were cultured in solid MS medium containing 2% sucrose and 1 mg/l 2,4-D.

Site-Directed mutagenesis

PCR-based site mutagenesis was carried out using as template the amplified coding sequence of *RIMA* in the pDONR207 vector. Primers (Supplemental Table 3) were phosphorylated in a reaction with T4 polynucleotide kinase enzyme. For PCR reaction, we used Phusion ® High-Fidelity DNA Polymerase (Thermo) following the manufacturer's protocol. The purified PCR product was ligated and transformed into DH5a *E. coli*.

Protein production for immunization

The *RIMA* coding sequence in the pDONR207 vector was used as template for inverse PCR with primers Flag F and RIMAc R (Supplemental Table 3) to obtain the N-terminal part of RIMA (amino acids 1-305) fused to Flag epitope tag in the pDONR207 vector. This construct was used for Gateway recombination-based cloning into the pDEST17 destination vector and transformed into *E. coli* strain BL21-CodonPlus. Cells were induced for protein expression overnight at 18ºC by adding 0.1 mM IPTG in LB culture medium supplemented with 100 mg/l carbenicillin and 2g/l glucose after reaching OD600=0.6. The cells were harvested at 3200 x *g* for 20 min at 4ºC, resuspended in 200 gl/l sucrose and frozen at -20ºC until use. The defrosted suspension was supplemented to reach a final concentration of 50 mM Tris-HCl (pH 7.5), 150 mM NaCl and protease inhibitors (Roche). Cells were disrupted by passing through a French Press and the suspension centrifuged at 20000 x *g* to remove cell debris. The supernatant was loaded onto a Ni-NTA (Clontech) column that was washed with 50 mM Tris-HCl (pH 7.5), 5% (v/v) glycerol, 150 mM NaCl, and eluted with the same buffer supplemented with 250 mM imidazole. The eluted fraction was passed through an anti-Flag resin (Sigma) column, and this was washed with the former wash buffer and eluted in the same buffer supplemented with 0.2 g/l Flag peptide. The soluble purified protein was used to immunize rabbits for antiserum production by Pineda Antibody-Services (Germany).

Co-immunoprecipitation

Plant material was ground in 4 ml extraction buffer (50 mM Tris-HCl, pH 7.5; 5% glycerol; 150 mM NaCl; 0.1% Triton X-100; 100 μM $ZnSO_4$; 2 mM DTT; 1 mM PMSF and protease inhibitors [Roche]) per gram of material and centrifuged at 20000 x *g* for 30 min. Protein concentration was adjusted using the Bradford method (Bio-rad). Co-immunoprecipitation mixtures were made containing the same amounts of total protein in the same volume. For immunoprecipitation protein G Dynabeads (Life Technologies) were used.

Microscopy analyses

For Nomarski microscopy, tissues were cleared in chloral hydrate and imaged with a Zeiss Axioskop microscope. For confocal microscopy, plants were monitored using a Leica TCS SP5 laser scanning confocal microscope with propidium iodide as counterstain. For GFP fluorescence quantification, single optical sections from roots of *ProRIMA:RIMA-GFP rima-1* plants were acquired with identical settings under sequential scanning to prevent signal bleed-through. The fields imaged were 125 μm x 125 μm (1024 x 1024 pixels). In cells of the elongation zone, nuclei were unequivocally distinguished from vacuoles by the weak propidium iodide labelling of the nucleolus. Mean GFP intensity per pixel within the nuclei, cytosol and vacuoles was measured using the FIJI software package.

Identification of IYO-interacting proteins using IP/MS-MS

Immunoprecipitation (IP) experiments were performed as described previously (Kaufmann et al., 2010) using 3 g of *Pro35S:IYO-GFP* or Wt seedlings for each sample. Interacting proteins were isolated by applying total protein extracts to anti-GFP coupled magnetic beads (Milteny Biotech). Three biological replicates of *Pro35S:IYO-GFP* were compared to three replicates of Wt controls (see Supplemental Table 1). Tandem mass spectrometry (MS) and statistical analysis using MaxQuant and Perseus software was performed as described previously (Lee and Young, 2013; Pijnappel et al., 2013).

Microarray analysis

For microarray analysis, seeds were sown in soil, vernalized for 2 days at 4ºC and grown in a growth chamber under a 14 h light: 10 h dark photoperiod for 32 days. Inflorescence shoot apices from 11 plants of each genotype were pooled in each experiment. Total RNA was extracted using Trizol (Invitrogen) and 4 biological replicates with pooled RNA from 3 independent experiments (12 independent experiments in total) were obtained for each genotype. Microarray profiles were obtained as described (Sanmartin et al., 2011). For co-expression analysis, we used the ACT tool that analyzes 322 ATH1 microarray hybridizations from the NASC/GARNet dataset covering a wide range of biological processes and conditions (Jen et al., 2006).

Flow Cytometry Analysis

Leaves from Wt and the callus-like *rima-2 iyo-1* plants were chopped with a razor blade in Galbraith's buffer (45 mM $MgCl_2$, 30 mM sodium citrate, 20 mM MOPS, 0.1% TritonX-100) (Galbraith et al., 1983) and filtered through a 30-µm nylon filter to remove tissue debris. DNA was stained with propidium iodide (50 mg/l) at 37ºC in darkness for 20 min prior to nuclear DNA content measurements in a Coulter Cytomics FC500 cytometer.

Accession numbers

Sequence data from this article can be found in the Arabidopsis Genome Initiative of GenBank/EMBL databases under the following accession numbers: *RIMA*: At5g26760; *IYO*: At4g38440; *GPN1*: At4g21800; *GPN2*: At5g22370. Microarray data from this article has been deposited at MIAMEXPRESS (GSE60169).

Supplemental Data

Supplemental Figure 1. Alignment of the zinc-finger domains from Arabidopsis RIMA, human RPAP2 and budding yeast RTR1.

Supplemental Figure 2. Characterization of antibodies against RIMA.

Supplemental Figure 3. IYO-GFP is excluded from nuclei of xylem pole pericycle cells.

Supplemental Figure 4. *ProIYO:IYO-GFP* is expressed in xylem pole pericycle cells but does not accumulate in the nucleus.

Supplemental Table 1. Overview of the IP-MS results.

Supplemental Table 2. Microarray expression data for a selected list of genes.

Supplemental Table 3. Primers used in this work

Acknowledgements

We thank P. Paredes for excellent technical assistance. This work was supported by the Spanish Ministry of Economy & Competitivity and FEDER funds (BIO2015-69582-P MINECO/FEDER to ER, MS and JJSS), by the Netherlands Organization for Scientific Research (NWO VIDI 864.13.001 to BDR and ERA-CAPS project EURO-PEC; 849.13.006 to DW), the Research Foundation Flanders (FWO G0D0515N and 12D1815 to BDR) and the European Research Council (Starting Grant “CELLPATTERN”, Contract no. 281573 to DW).

Author Contributions

A.M, S.M, M.P. G-G, R. C., Mi. S, B. DeR., D. W., M.S and E.R performed research; J.J. S-S, M.S and E.R designed the research; M.S and E.R wrote the manuscript.

REFERENCES

Atta, R., Laurens, L., Boucheron-Dubuisson, E., Guivarc'h, A., Carnero, E., Giraudat-Pautot, V., Rech, P., and Chriqui, D. (2009). Pluripotency of

622 Arabidopsis xylem pericycle underlies shoot regeneration from root and
623 hypocotyl explants grown in vitro. Plant J **57,** 626-644.
624 **Beeckman, T., Burssens, S., and Inze, D.** (2001). The peri-cell-cycle in
625 Arabidopsis. J Exp Bot **52,** 403-411.
626 **Benfey, P.N.** (2016). Defining the Path from Stem Cells to Differentiated Tissue.
627 Curr Top Dev Biol **116,** 35-43.
628 **Boulon, S., Pradet-Balade, B., Verheggen, C., Molle, D., Boireau, S.,**
629 **Georgieva, M., Azzag, K., Robert, M.C., Ahmad, Y., Neel, H., Lamond,**
630 **A.I., and Bertrand, E.** (2010). HSP90 and its R2TP/Prefoldin-like
631 cochaperone are involved in the cytoplasmic assembly of RNA polymerase
632 II. Mol Cell **39,** 912-924.
633 **Brookes, E., de Santiago, I., Hebenstreit, D., Morris, K.J., Carroll, T., Xie, S.Q.,**
634 **Stock, J.K., Heidemann, M., Eick, D., Nozaki, N., Kimura, H., Ragoussis,**
635 **J., Teichmann, S.A., and Pombo, A.** (2012). Polycomb associates
636 genome-wide with a specific RNA polymerase II variant, and regulates
637 metabolic genes in ESCs. Cell Stem Cell **10,** 157-170.
638 **Calera, M.R., Zamora-Ramos, C., Araiza-Villanueva, M.G., Moreno-Aguilar,**
639 **C.A., Pena-Gomez, S.G., Castellanos-Teran, F., Robledo-Rivera, A.Y.,**
640 **and Sanchez-Olea, R.** (2011). Parcs/Gpn3 is required for the nuclear
641 accumulation of RNA polymerase II. Biochim Biophys Acta **1813,** 1708-
642 1716.
643 **Carre, C., and Shiekhattar, R.** (2011). Human GTPases associate with RNA
644 polymerase II to mediate its nuclear import. Mol Cell Biol **31,** 3953-3962.
645 **Che, P., Lall, S., and Howell, S.H.** (2007). Developmental steps in acquiring
646 competence for shoot development in Arabidopsis tissue culture. Planta
647 **226,** 1183-1194.
648 **Cheng, Y., Cao, L., Wang, S., Li, Y., Shi, X., Liu, H., Li, L., Zhang, Z., Fowke,**
649 **L.C., Wang, H., and Zhou, Y.** (2015). Downregulation of multiple CDK
650 inhibitor ICK/KRP genes upregulates the E2F pathway and increases cell
651 proliferation, and organ and seed sizes in Arabidopsis. Plant J **75,** 642-655.

Chupeau, M.C., Granier, F., Pichon, O., Renou, J.P., Gaudin, V., and Chupeau, Y. (2013). Characterization of the early events leading to totipotency in an Arabidopsis protoplast liquid culture by temporal transcript profiling. Plant Cell **25,** 2444-2463.

DiDonato, R.J., Arbuckle, E., Buker, S., Sheets, J., Tobar, J., Totong, R., Grisafi, P., Fink, G.R., and Celenza, J.L. (2004). Arabidopsis ALF4 encodes a nuclear-localized protein required for lateral root formation. Plant J **37,** 340-353.

Dubrovsky, J.G., Doerner, P.W., Colon-Carmona, A., and Rost, T.L. (2000). Pericycle cell proliferation and lateral root initiation in Arabidopsis. Plant Physiol **124,** 1648-1657.

Egloff, S., Zaborowska, J., Laitem, C., Kiss, T., and Murphy, S. (2012). Ser7 phosphorylation of the CTD recruits the RPAP2 Ser5 phosphatase to snRNA genes. Mol Cell **45,** 111-122.

Fan, M., Xu, C., Xu, K., and Hu, Y. (2012). LATERAL ORGAN BOUNDARIES DOMAIN transcription factors direct callus formation in Arabidopsis regeneration. Cell Res **22,** 1169-1180.

Forget, D., Lacombe, A.A., Cloutier, P., Lavallee-Adam, M., Blanchette, M., and Coulombe, B. (2013). Nuclear import of RNA polymerase II is coupled with nucleocytoplasmic shuttling of the RNA polymerase II-associated protein 2. Nucleic Acids Res **41,** 6881-6891.

Forget, D., Lacombe, A.A., Cloutier, P., Al-Khoury, R., Bouchard, A., Lavallee-Adam, M., Faubert, D., Jeronimo, C., Blanchette, M., and Coulombe, B. (2010). The protein interaction network of the human transcription machinery reveals a role for the conserved GTPase RPAP4/GPN1 and microtubule assembly in nuclear import and biogenesis of RNA polymerase II. Mol Cell Proteomics **9,** 2827-2839.

Fukaki, H., Okushima, Y., and Tasaka, M. (2007). Auxin-mediated lateral root formation in higher plants. Int Rev Cytol **256,** 111-137.

Fukaki, H., Tameda, S., Masuda, H., and Tasaka, M. (2002). Lateral root formation is blocked by a gain-of-function mutation in the SOLITARY-ROOT/IAA14 gene of Arabidopsis. Plant J **29,** 153-168.

Gaillochet, C., and Lohmann, J.U. (2015). The never-ending story: from pluripotency to plant developmental plasticity. Development **142,** 2237-2249.

Galbraith, D.W., Harkins, K.R., Maddox, J.M., Ayres, N.M., Sharma, D.P., and Firoozabady, E. (1983). Rapid flow cytometric analysis of the cell cycle in intact plant tissues. Science **220,** 1049-1051.

Giaever, G., Chu, A.M., Ni, L., Connelly, C., Riles, L., Veronneau, S., Dow, S., Lucau-Danila, A., Anderson, K., Andre, B., Arkin, A.P., Astromoff, A., El-Bakkoury, M., Bangham, R., Benito, R., Brachat, S., Campanaro, S., Curtiss, M., Davis, K., Deutschbauer, A., Entian, K.D., Flaherty, P., Foury, F., Garfinkel, D.J., Gerstein, M., Gotte, D., Guldener, U., Hegemann, J.H., Hempel, S., Herman, Z., Jaramillo, D.F., Kelly, D.E., Kelly, S.L., Kotter, P., LaBonte, D., Lamb, D.C., Lan, N., Liang, H., Liao, H., Liu, L., Luo, C., Lussier, M., Mao, R., Menard, P., Ooi, S.L., Revuelta, J.L., Roberts, C.J., Rose, M., Ross-Macdonald, P., Scherens, B., Schimmack, G., Shafer, B., Shoemaker, D.D., Sookhai-Mahadeo, S., Storms, R.K., Strathern, J.N., Valle, G., Voet, M., Volckaert, G., Wang, C.Y., Ward, T.R., Wilhelmy, J., Winzeler, E.A., Yang, Y., Yen, G., Youngman, E., Yu, K., Bussey, H., Boeke, J.D., Snyder, M., Philippsen, P., Davis, R.W., and Johnston, M. (2002). Functional profiling of the Saccharomyces cerevisiae genome. Nature **418,** 387-391.

Gibney, P.A., Fries, T., Bailer, S.M., and Morano, K.A. (2008). Rtr1 is the Saccharomyces cerevisiae homolog of a novel family of RNA polymerase II-binding proteins. Eukaryot Cell **7,** 938-948.

Gomez-Navarro, N., and Estruch, F. (2015). Different pathways for the nuclear import of yeast RNA polymerase II. Biochim Biophys Acta **1849,** 1354-1362.

Guenther, M.G., Levine, S.S., Boyer, L.A., Jaenisch, R., and Young, R.A. (2007). A chromatin landmark and transcription initiation at most promoters in human cells. Cell **130,** 77-88.

Haasen, D., Kohler, C., Neuhaus, G., and Merkle, T. (1999). Nuclear export of proteins in plants: AtXPO1 is the export receptor for leucine-rich nuclear export signals in Arabidopsis thaliana. Plant J **20,** 695-705.

Hsu, P.L., Yang, F., Smith-Kinnaman, W., Yang, W., Song, J.E., Mosley, A.L., and Varani, G. (2014). Rtr1 Is a Dual Specificity Phosphatase That Dephosphorylates Tyr1 and Ser5 on the RNA Polymerase II CTD. J Mol Biol **426,** 2970-2981.

Hunter, G.O., Fox, M.J., Smith-Kinnaman, W.R., Gogol, M., Fleharty, B., and Mosley, A.L. (2016). Phosphatase Rtr1 Regulates Global Levels of Serine 5 RNA Polymerase II C-Terminal Domain Phosphorylation and Cotranscriptional Histone Methylation. Mol Cell Biol **36,** 2236-2245.

Ikeuchi, M., Sugimoto, K., and Iwase, A. (2013). Plant callus: mechanisms of induction and repression. Plant Cell **25,** 3159-3173.

Ikeuchi, M., Iwase, A., Rymen, B., Harashima, H., Shibata, M., Ohnuma, M., Breuer, C., Morao, A.K., de Lucas, M., De Veylder, L., Goodrich, J., Brady, S.M., Roudier, F., and Sugimoto, K. (2015). PRC2 represses dedifferentiation of mature somatic cells in Arabidopsis. Nat Plants **1,** 15089.

Irani, S., Yogesha, S.D., Mayfield, J., Zhang, M., Zhang, Y., Matthews, W.L., Nie, G., Prescott, N.A., and Zhang, Y.J. (2016). Structure of Saccharomyces cerevisiae Rtr1 reveals an active site for an atypical phosphatase. Sci Signal **9,** ra24.

Iwase, A., Ohme-Takagi, M., and Sugimoto, K. (2011a). WIND1: a key molecular switch for plant cell dedifferentiation. Plant Signal Behav **6,** 1943-1945.

Iwase, A., Mitsuda, N., Koyama, T., Hiratsu, K., Kojima, M., Arai, T., Inoue, Y., Seki, M., Sakakibara, H., Sugimoto, K., and Ohme-Takagi, M. (2011b). The AP2/ERF transcription factor WIND1 controls cell dedifferentiation in Arabidopsis. Curr Biol **21,** 508-514.

Jen, C.H., Manfield, I.W., Michalopoulos, I., Pinney, J.W., Willats, W.G., Gilmartin, P.M., and Westhead, D.R. (2006). The Arabidopsis co-expression tool (ACT): a WWW-based tool and database for microarray-based gene expression analysis. Plant J **46,** 336-348.

Jeronimo, C., Forget, D., Bouchard, A., Li, Q., Chua, G., Poitras, C., Therien, C., Bergeron, D., Bourassa, S., Greenblatt, J., Chabot, B., Poirier, G.G., Hughes, T.R., Blanchette, M., Price, D.H., and Coulombe, B. (2007). Systematic analysis of the protein interaction network for the human transcription machinery reveals the identity of the 7SK capping enzyme. Mol Cell **27,** 262-274.

Jeronimo, C., Langelier, M.F., Zeghouf, M., Cojocaru, M., Bergeron, D., Baali, D., Forget, D., Mnaimneh, S., Davierwala, A.P., Pootoolal, J., Chandy, M., Canadien, V., Beattie, B.K., Richards, D.P., Workman, J.L., Hughes, T.R., Greenblatt, J., and Coulombe, B. (2004). RPAP1, a novel human RNA polymerase II-associated protein affinity purified with recombinant wild-type and mutated polymerase subunits. Mol Cell Biol **24,** 7043-7058.

Kaufmann, K., Pajoro, A., and Angenent, G.C. (2010). Regulation of transcription in plants: mechanisms controlling developmental switches. Nat Rev Genet **11,** 830-842.

Lahmy, S., Guilleminot, J., Schmit, A.C., Pelletier, G., Chaboute, M.E., and Devic, M. (2007). QQT proteins colocalize with microtubules and are essential for early embryo development in Arabidopsis. Plant J **50,** 615-626.

Lee, H.W., Kim, N.Y., Lee, D.J., and Kim, J. (2009). LBD18/ASL20 regulates lateral root formation in combination with LBD16/ASL18 downstream of ARF7 and ARF19 in Arabidopsis. Plant Physiol **151,** 1377-1389.

Lee, T.I., and Young, R.A. (2013). Transcriptional regulation and its misregulation in disease. Cell **152,** 1237-1251.

Liu, J., Sheng, L., Xu, Y., Li, J., Yang, Z., Huang, H., and Xu, L. (2014). WOX11 and 12 are involved in the first-step cell fate transition during de novo root organogenesis in Arabidopsis. Plant Cell **26,** 1081-1093.

Minaker, S.W., Filiatrault, M.C., Ben-Aroya, S., Hieter, P., and Stirling, P.C. (2013). Biogenesis of RNA polymerases II and III requires the conserved GPN small GTPases in Saccharomyces cerevisiae. Genetics **193,** 853-864.

Mosley, A.L., Pattenden, S.G., Carey, M., Venkatesh, S., Gilmore, J.M., Florens, L., Workman, J.L., and Washburn, M.P. (2009). Rtr1 is a CTD phosphatase that regulates RNA polymerase II during the transition from serine 5 to serine 2 phosphorylation. Mol Cell **34,** 168-178.

Ni, Z., Xu, C., Guo, X., Hunter, G.O., Kuznetsova, O.V., Tempel, W., Marcon, E., Zhong, G., Guo, H., Kuo, W.H., Li, J., Young, P., Olsen, J.B., Wan, C., Loppnau, P., El Bakkouri, M., Senisterra, G.A., He, H., Huang, H., Sidhu, S.S., Emili, A., Murphy, S., Mosley, A.L., Arrowsmith, C.H., Min, J., and Greenblatt, J.F. (2014). RPRD1A and RPRD1B are human RNA polymerase II C-terminal domain scaffolds for Ser5 dephosphorylation. Nat Struct Mol Biol **21,** 686-695.

Niesser, J., Wagner, F.R., Kostrewa, D., Muhlbacher, W., and Cramer, P. (2016). Structure of GPN-Loop GTPase Npa3 and Implications for RNA Polymerase II Assembly. Mol Cell Biol **36,** 820-831.

Okushima, Y., Fukaki, H., Onoda, M., Theologis, A., and Tasaka, M. (2007). ARF7 and ARF19 regulate lateral root formation via direct activation of LBD/ASL genes in Arabidopsis. Plant Cell **19,** 118-130.

Perianez-Rodriguez, J., Manzano, C., and Moreno-Risueno, M.A. (2014). Post-embryonic organogenesis and plant regeneration from tissues: two sides of the same coin? Front Plant Sci **5,** 219.

Pijnappel, W.W., Esch, D., Baltissen, M.P., Wu, G., Mischerikow, N., Bergsma, A.J., van der Wal, E., Han, D.W., Bruch, H., Moritz, S., Lijnzaad, P., Altelaar, A.F., Sameith, K., Zaehres, H., Heck, A.J., Holstege, F.C., Scholer, H.R., and Timmers, H.T. (2013). A central role for TFIID in the pluripotent transcription circuitry. Nature **495,** 516-519.

Sablowski, R. (2011). Plant stem cell niches: from signalling to execution. Curr Opin Plant Biol **14,** 4-9.

Sablowski, R. (2015). Control of patterning, growth, and differentiation by floral organ identity genes. J Exp Bot **66,** 1065-1073.

Sanchez Alvarado, A., and Yamanaka, S. (2014). Rethinking differentiation: stem cells, regeneration, and plasticity. Cell **157,** 110-119.

Sanmartin, M., Sauer, M., Munoz, A., and Rojo, E. (2012). MINIYO and transcriptional elongation: lifting the roadblock to differentiation. Transcription **3,** 25-28.

Sanmartin, M., Sauer, M., Munoz, A., Zouhar, J., Ordonez, A., van de Ven, W.T., Caro, E., de la Paz Sanchez, M., Raikhel, N.V., Gutierrez, C., Sanchez-Serrano, J.J., and Rojo, E. (2011). A molecular switch for initiating cell differentiation in Arabidopsis. Curr Biol **21,** 999-1008.

Sanz, L., Dewitte, W., Forzani, C., Patell, F., Nieuwland, J., Wen, B., Quelhas, P., De Jager, S., Titmus, C., Campilho, A., Ren, H., Estelle, M., Wang, H., and Murray, J.A. (2011). The Arabidopsis D-type cyclin CYCD2;1 and the inhibitor ICK2/KRP2 modulate auxin-induced lateral root formation. Plant Cell **23,** 641-660.

Scheres, B. (2007). Stem-cell niches: nursery rhymes across kingdoms. Nat Rev Mol Cell Biol **8,** 345-354.

Sena, G., Wang, X., Liu, H.Y., Hofhuis, H., and Birnbaum, K.D. (2009). Organ regeneration does not require a functional stem cell niche in plants. Nature **457,** 1150-1153.

Shang, B., Xu, C., Zhang, X., Cao, H., Xin, W., and Hu, Y. (2016). Very-long-chain fatty acids restrict regeneration capacity by confining pericycle competence for callus formation in Arabidopsis. Proc Natl Acad Sci U S A **113,** 5101-5106.

Staresincic, L., Walker, J., Dirac-Svejstrup, A.B., Mitter, R., and Svejstrup, J.Q. (2011). GTP-dependent binding and nuclear transport of RNA polymerase II by Npa3 protein. J Biol Chem **286,** 35553-35561.

Stock, J.K., Giadrossi, S., Casanova, M., Brookes, E., Vidal, M., Koseki, H., Brockdorff, N., Fisher, A.G., and Pombo, A. (2007). Ring1-mediated

ubiquitination of H2A restrains poised RNA polymerase II at bivalent genes in mouse ES cells. Nat Cell Biol **9,** 1428-1435.

Su, Y.H., and Zhang, X.S. (2014). The hormonal control of regeneration in plants. Curr Top Dev Biol **108,** 35-69.

Sugimoto, K., Jiao, Y., and Meyerowitz, E.M. (2010). Arabidopsis regeneration from multiple tissues occurs via a root development pathway. Dev Cell **18,** 463-471.

Sugimoto, K., Gordon, S.P., and Meyerowitz, E.M. (2011). Regeneration in plants and animals: dedifferentiation, transdifferentiation, or just differentiation? Trends Cell Biol **21,** 212-218.

Sugiyama, M. (2015). Historical review of research on plant cell dedifferentiation. J Plant Res **128,** 349-359.

Van Lijsebettens, M., and Grasser, K.D. (2014). Transcript elongation factors: shaping transcriptomes after transcript initiation. Trends Plant Sci **19,** 717-726.

Wani, S., Hirose, Y., and Ohkuma, Y. (2014). Human RNA polymerase II-associated protein 2 (RPAP2) interacts directly with the RNA polymerase II subunit Rpb6 and participates in pre-mRNA 3'-end formation. Drug Discov Ther **8,** 255-261.

Wolters, H., and Jurgens, G. (2009). Survival of the flexible: hormonal growth control and adaptation in plant development. Nat Rev Genet **10,** 305-317.

Xiang, K., Manley, J.L., and Tong, L. (2012). The yeast regulator of transcription protein Rtr1 lacks an active site and phosphatase activity. Nat Commun **3,** 946.

Young, R.A. (2011). Control of the embryonic stem cell state. Cell **144,** 940-954.

Zhang, T.Q., Lian, H., Tang, H., Dolezal, K., Zhou, C.M., Yu, S., Chen, J.H., Chen, Q., Liu, H., Ljung, K., and Wang, J.W. (2015). An intrinsic microRNA timer regulates progressive decline in shoot regenerative capacity in plants. Plant Cell **27,** 349-360.

FIGURE LEGENDS

Figure 1. IYO interacts with GPN proteins and RIMA. (A) BiFC assay with the N-terminal half of YFP fused to IYO (*N-IYO*) and the C-terminal half of YFP fused to GPN1 (*GPN1-C*) or GPN2 (*GPN2-C*). (B) BiFC assay with the C-terminal half of YFP fused to IYO (*C-IYO*) and the N-terminal half of YFP fused to RIMA (*N-RIMA*). (C) BiFC assay with the C-terminal half of YFP fused to IYO (*C-IYO*) and the N-terminal half of YFP fused to Wt RIMA (*N-RIMA*) or to the C56A/C61A (*N-56/61*) or C94A/C98A (*N-94/98*) RIMA mutant construct. Immunoblotting verified expression of all constructs in the assays. The arrowhead marks the position of C-IYO and the arrow the position of N-RIMA, N-56/61 and N-94/98. Scale bar: 25 μm. (D) Total protein sample from 12-day-old *Pro35S:IYO-HA* transgenic seedlings (Input) was immunoprecipitated with anti-RIMA antibodies (a-RIMA) or preimmune serum from the same rabbit (Preimm) and aliquots were analyzed by immunoblots with anti-HA and anti-RIMA antibodies (low exposure image on top to show RIMA specifically immunopurified with the immune serum and long exposure image below to show RIMA in the input). Coomassie staining of the blots showed lack of contamination with Rubisco in the immunopurified fractions. Scale bars: 25 μm.

Figure 2. *RIMA* is expressed in meristems and organ primordia. (A-B) β-glucuronidase activity in the aerial organs (A) and roots (B) of *ProRIMA:GUS* plants. Scale bar: 1 mm (top-left panel), 50 μm (additional panels). (C) Confocal images of roots from a *rima-1* mutant complemented with *ProRIMA:RIMA-GFP*. Green signal: GFP; Red signal: propidium iodide. Scale bar: 50 μm. (D) Confocal images of epidermal cells from the meristematic (top panel) and the elongation zone (bottom panel) of a root from a *ProRIMA:RIMA-GFP rima-1* plant. Scale bar: 10 μm. (E) Mean GFP fluorescence intensity in the cytosol and in the nucleus of epidermal cells from the elongation zone of primary roots from *ProRIMA:RIMA-GFP rima-1* plants. The average local background signal (measured in vacuoles from the same cells) was subtracted from the values. a. u.: artificial units. The standard deviation (error bars) and the p-values (unpaired t-test for the null

892 hypothesis that fluorescence is not above background levels) are shown above the
893 graphs. (F) Confocal image of *Nicotiana benthamiana* leaf epidermal cells
894 transiently transformed with *Pro35S:RIMA-GFP* and mock treated (-LMB) or
895 incubated with 0.9 μM Leptomycin B (+LMB) for 2 h. Arrowhead marks a nucleus
896 with low internal fluorescence and arrow a nucleus with high internal fluorescence.
897 Scale bar: 25 μm. (G) Confocal images of roots from *ProRIMA:RIMA-GFP* plants
898 mock treated (-LMB) or incubated with 0.9 μM LMB for 2.5 hours (+LMB). Insets
899 show details of nuclei from the roots shown on the left. Scale bar: 10 μm.
900
901 **Figure 3. *RIMA* is required for cell differentiation.** (A) Nomarski images of
902 cleared seeds from siliques of heterozygous *rima-1/RIMA* plants. The *rima-1*
903 mutant embryos and the corresponding Wt or heterozygous sibling (Wt) from the
904 same silique at torpedo stage (left panels) and mature stage (right panels) are
905 shown. Scale bar: 25 μm. (B) Images of 10-day-old (upper panels) and 30-day-old
906 (lower panels) Wt and *rima-2* plants. Scale bar: 1 mm. (C) Expression of the
907 *ProSTM:GUS* shoot meristem marker in 5-day-old seedlings. Scale bar: 100 μm.
908 (D) Images of the primary stem from a *rima-2* plant. All *rima-2* plants developed
909 fasciated meristems with split primary SAMs. Scale bar: 1 mm. Upper inset shows
910 enlarged image of a duplicated flower and lower inset shows a duplicated silique
911 from a *rima-2* plant (on average there were more than one duplicated flower per
912 plant, n=150 plants). (E) Images of the cotyledon epidermis from 6-day-old
913 seedlings. The *rima-2* mutant retains small protoderm-like cells that express the
914 *ProTMM: TMM-GFP* marker. Scale bar: 25 μm. Inset shows cluster of stomata in
915 cotyledons of 10-day-old *rima-2* plants. Scale bar: 12.5 μm. (F) Images of cleared
916 root apical meristems from 5-day-old Wt and *rima-2* plants. Cell tracings of the files
917 marked with the brackets are shown to highlight the ectopic periclinal divisions in
918 the mutant. Arrow: quiescent center. Scale bar: 25 μm. (G) Expression of the
919 *J2341* columella initials marker in 5-day-old seedlings. Arrow: quiescent center.
920 Scale bar: 20 μm. (H) Northern analysis of RNA samples from inflorescences of Wt
921 and *rima-2* plants. The arrowhead marks the full-length *RIMA* transcript and the
922 asterisk marks a truncated transcript that accumulates in the mutant. rRNA is

shown as a loading control. (I) Images of 14-day-old (upper panels) and 60-day-old (lower panels) *rima-2* and *rima-1/rima-2* plants. Scale bar: 1 mm. (J) Aerial view of a 12-day-old Wt plant, a *rima-2* mutant, and two representative lines of *rima-1* transformed with *ProRIMA:RIMA-GFP* or *Pro35S:RIMA-GFP*. In the lower panel, the expression level of the transgenes in each of the genotypes from the top panel was determined by immunoblot with anti-GFP antibodies. (K) Two examples of twin globular embryos formed in seeds from a representative line of *rima-1* transformed with *Pro35S:RIMA-GFP* (5% of seeds had twin embryos, n=162). Scale bar: 25 μm.

Figure 4. *IYO* and *RIMA* activate transcription of common developmental programs. (A) Venn diagram analysis of the overlap between the sets of 400 genes most down-regulated in *iyo-1*/Wt (down *iyo-1*) and *rima-2*/Wt (down *rima-2*) inflorescences. The p-value (Hypergeometric test) for the observed level of overlap is shown above the graphs. (B) Graphical display of microarray expression data (log_2 of the expression ratio) in Wt versus *iyo-1* (Wt/*iyo-1*) and Wt versus *rima-2* (*Wt/rima-2*) of the 400 genes most highly down-regulated in *iyo-1* inflorescences (Sanmartin et al., 2011). (C) GSEA analysis of gene sets significantly down-regulated in *iyo-1*/Wt and *rima-2*/Wt inflorescence apices.

Figure 5. *IYO* and *RIMA* interact genetically to activate differentiation. (A) Images of 10-day-old plants (genotypes as indicated in the panels). A magnification of the framed *iyo-1 rima-2* seedling is shown on the right panel. Scale bar: 0.5 mm. (B) 80-day-old *iyo-1 rima-2* plant. Scale bar: 2 mm. (C) Flow cytometry analysis of nuclear DNA content in 45-day-old *iyo-1 rima-2* mutants. The DNA content of the first pair of leaves from 18-day-old wild-type plants is shown for comparison. (D) Images from 11-day-old plants (genotypes as indicated in the panels). Scale bar: 1mm.

Figure 6. RIMA is required for IYO nuclear accumulation and for its pro-differentiation activity. (A) Confocal images of roots from a *ProIYO:IYO-GFP* line

in a Wt background or introgressed into a *rima-2* mutant background (*rima-2*) mock treated (-LMB) or incubated with 0.9 μM LMB for 2.5 hours (+LMB). Scale bar: 50 μm. (B) Confocal images of *N. benthamiana* leaf epidermal cells transiently transformed with *Pro35S:RIMA-GFP* alone or together with *Pro35S:IYO-HA*. Arrowheads mark nuclei with low internal fluorescence and arrows nuclei with high internal fluorescence. Scale bar: 25 μm. (C) Images of 14-day-old *rima-2*, *Pro35S:IYO-HA*, and *Pro35S:IYO-HA rima-2* plants. Scale bar: 1 mm. In the lower panel, IYO-HA expression in plants from the genotypes shown was determined by immunoblotting with anti-HA antibodies.

Figure 7. Overexpression of *IYO* and *RIMA* blocks callus formation (A-B) Confocal images of *Pro35S:IYO-GFP* and *Pro35S:RPB10-GFP* plants. Note that root development and RAM size in the transgenic *Pro35S:IYO-GFP* line was indistinguishable from *Pro35S:RPB10-GFP* and Wt plants. (A) Single confocal longitudinal sections at the equatorial plane containing the two xylem poles of roots from 5-day-old plants (top panels). Orthogonal views of the roots reconstructed from serial sections are shown in the bottom panels. The positions of the orthogonal sections are marked on the top panels. Asterisks mark GFP positive nuclei from the xylem pole pericycle. Nuclei from other cell layers are identified by the letters. ep: epidermis; c: cortex; e: endodermis; v: vasculature; Scale bar: 25 μm. (B) Confocal images from roots of 6-day-old plants treated for 3 days in liquid MS medium containing 300 ng/ml of 2,4D. Scale bar: 50 μm. (C-E) Images from *Pro35S:RIMA-GFP, Pro35S:IYO-HA* and *Pro35S:RIMA-GFP Pro35S:IYO-HA* double transgenic plants. Note that Wt plants were indistinguishable from *Pro35S:RIMA-GFP* plants and are not shown. (C) Roots from 14-day-old plants. Scale bar: 1 mm. Inset shows a Nomarski image of the only root primordia emerged in a *Pro35S:RIMA-GFP Pro35S:IYO-HA* plant. Scale bar: 50 μm (D) Nomarski images of sections from the mature zone of the root from 24-day-old plants cultured for 5 days in callus-inducing medium. Red bars mark pericycle domains where periclinal divisions have taken place. Scale bar: 25 μm. (E) Images

984 of sections from the mature zone of the root from 24-day-old plants cultured for 41
985 days in callus-inducing medium. Scale bar: 1 mm.
986

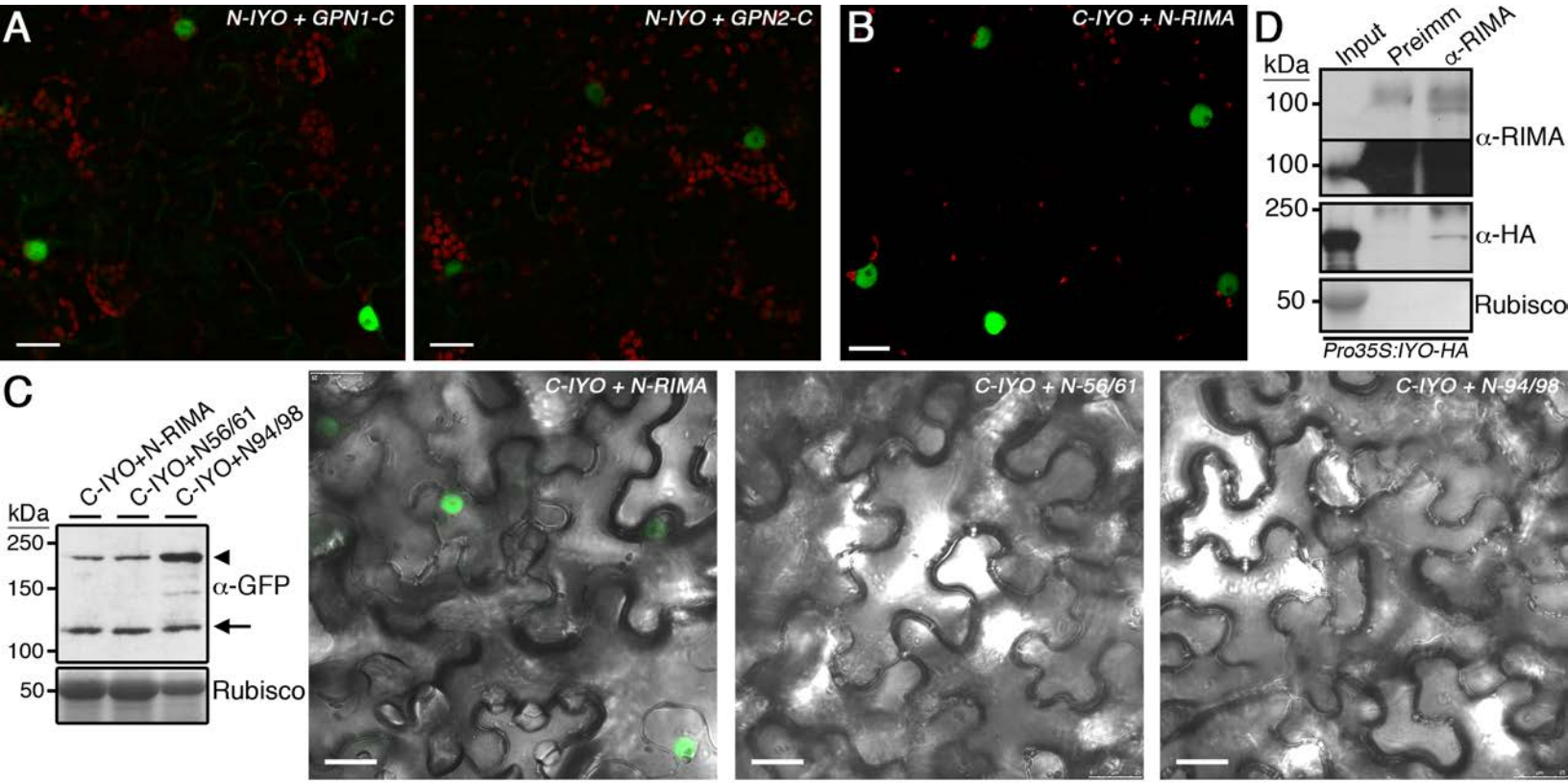

Figure 1. IYO interacts with GPN proteins and RIMA. (A) BiFC assay with the N-terminal half of YFP fused to IYO (*N-IYO*) and the C-terminal half of YFP fused to GPN1 (*GPN1-C*) or GPN2 (*GPN2-C*). (B) BiFC assay with the C-terminal half of YFP fused to IYO (*C-IYO*) and the N-terminal half of YFP fused to RIMA (*N-RIMA*). (C) BiFC assay with the C-terminal half of YFP fused to IYO (*C-IYO*) and the N-terminal half of YFP fused to Wt RIMA (*N-RIMA*) or to the C56A/C61A (*N-56/61*) or C94A/C98A (*N-94/98*) RIMA mutant construct. Immunoblotting verified expression of all constructs in the assays. The arrowhead marks the position of C-IYO and the arrow the position of N-RIMA, N-56/61 and N-94/98. Scale bar: 25 μm. (D) Total protein sample from 12-day-old *Pro35S:IYO-HA* transgenic seedlings (Input) was immunoprecipitated with anti-RIMA antibodies (α–RIMA) or preimmune serum from the same rabbit (Preimm) and aliquots were analyzed by immunoblots with anti-HA and anti-RIMA antibodies (low exposure image on top to show RIMA specifically immunopurified with the immune serum and long exposure image below to show RIMA in the input). Coomassie staining of the blots showed lack of contamination with Rubisco in the immunopurified fractions. Scale bars: 25 μm.

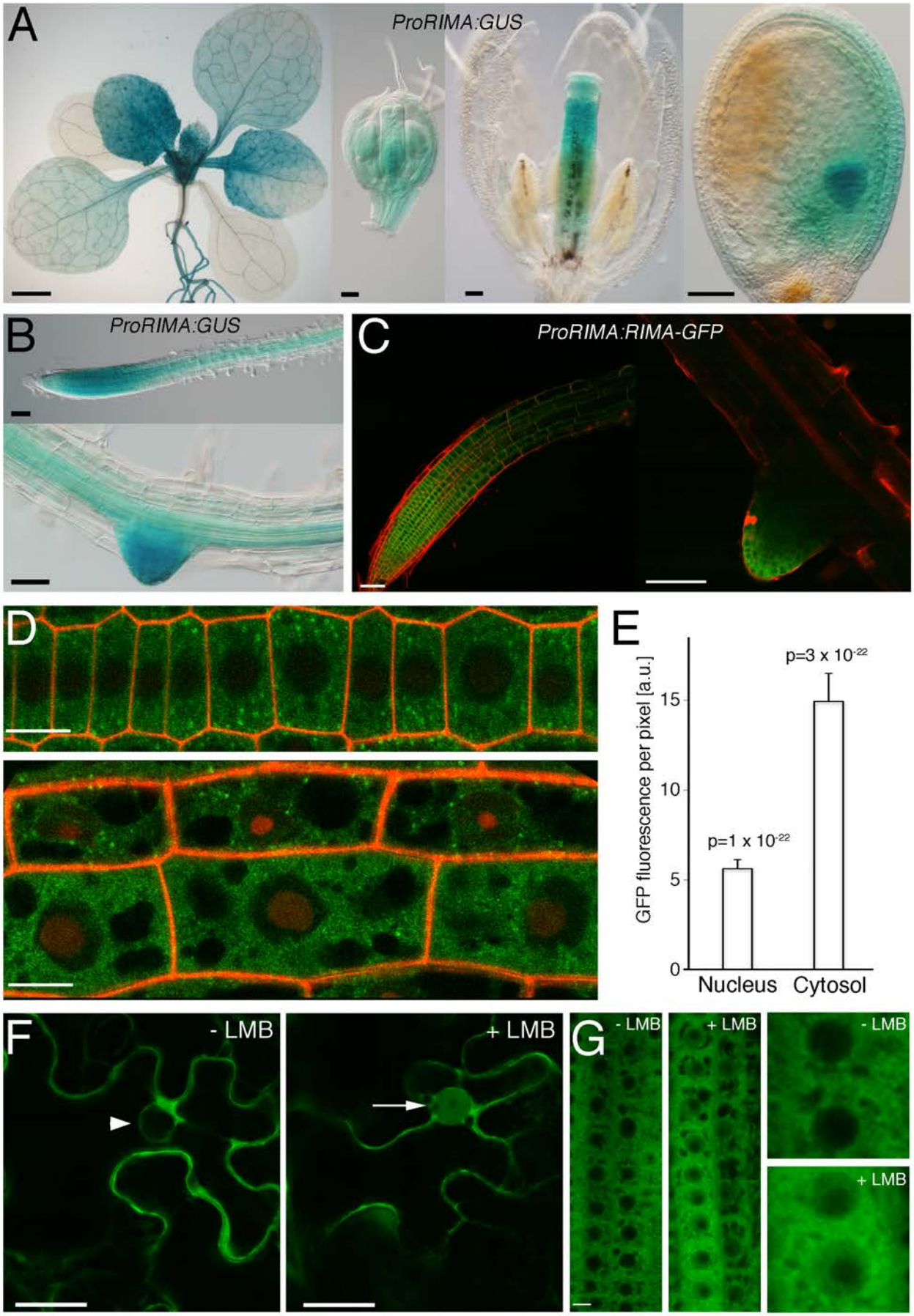

Figure 2. *RIMA* is expressed in meristems and organ primordia. (A-B) β-glucuronidase activity in the aerial organs (A) and roots (B) of *ProRIMA:GUS* plants. Scale bar: 1 mm (top-left panel), 50 μm (additional panels). (C) Confocal images of roots from a *rima-1* mutant complemented with *ProRIMA:RIMA-GFP*. Green signal: GFP; Red signal: propidium iodide. Scale bar: 50 μm. (D) Confocal images of epidermal cells from the meristematic (top panel) and the elongation zone (bottom panel) of a root from a *ProRIMA:RIMA-GFP rima-1* plant. Scale bar: 10 μm. (E) Mean GFP fluorescence intensity in the cytosol and in the nucleus of epidermal cells from the elongation zone of primary roots from *ProRIMA:RIMA-GFP rima-1* plants. The average local background signal (measured in vacuoles from the same cells) was subtracted from the values. a. u.: artificial units. The standard deviation (error bars) and the p-values (unpaired t-test for the null hypothesis that fluorescence is not above background levels) are shown above the graphs. (F) Confocal image of *Nicotiana benthamiana* leaf epidermal cells transiently transformed with *Pro35S:RIMA-GFP* and mock treated (-LMB) or incubated with 0.9 μM Leptomycin B (+LMB) for 2 h. Arrowhead marks a nucleus with low internal fluorescence and arrow a nucleus with high internal fluorescence. Scale bar: 25 μm. (G) Confocal images of roots from *ProRIMA:RIMA-GFP* plants mock treated (-LMB) or incubated with 0.9 μM LMB for 2.5 hours (+LMB). Insets show details of nuclei from the roots shown on the left. Scale bar: 10 μm.

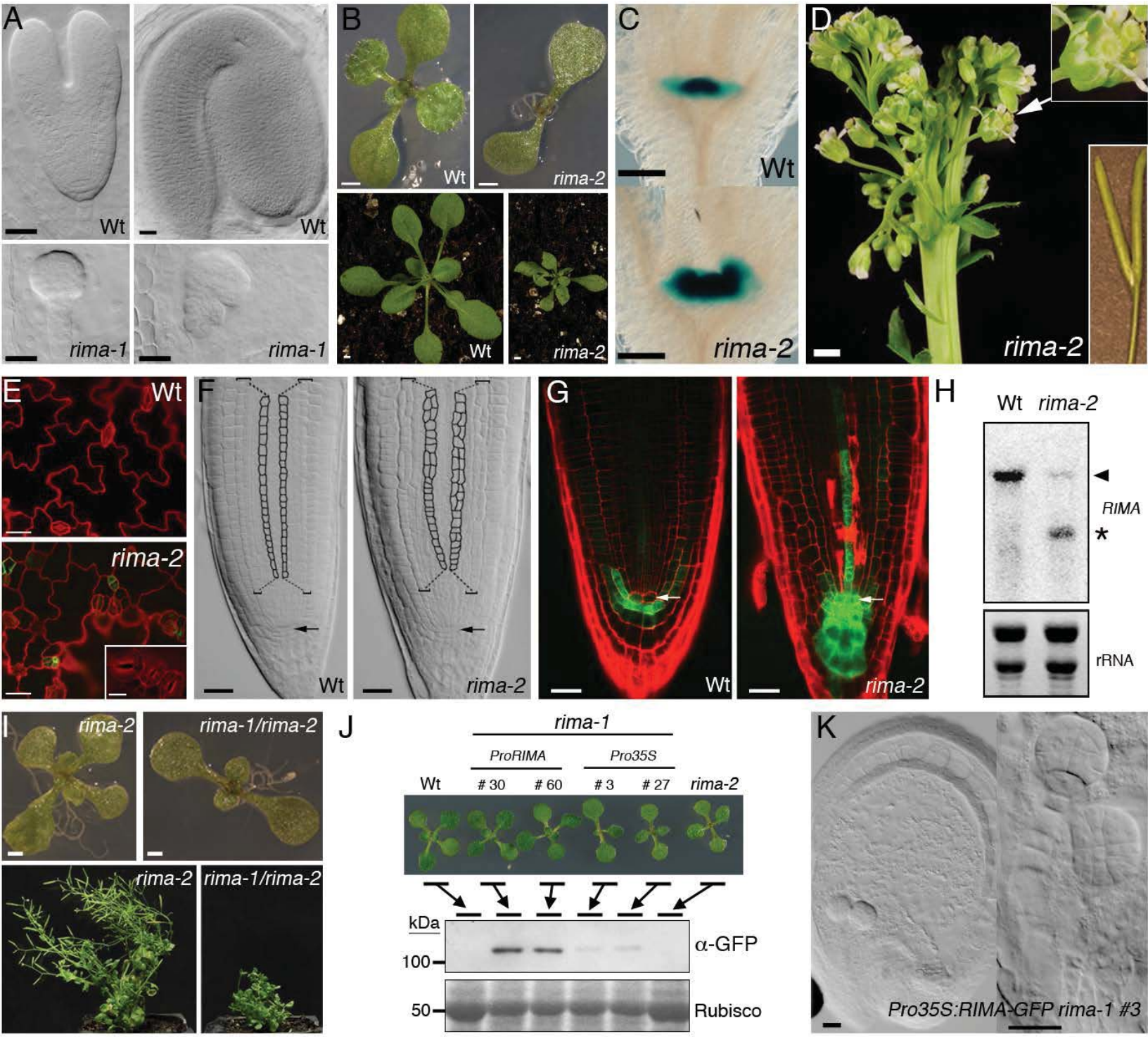

Figure 3. *RIMA* is required for cell differentiation. (A) Nomarski images of cleared seeds from siliques of heterozygous *rima-1/RIMA* plants. The *rima-1* mutant embryos and the corresponding Wt or heterozygous sibling (Wt) from the same silique at torpedo stage (left panels) and mature stage (right panels) are shown. Scale bar: 25 μm. (B) Images of 10-day-old (upper panels) and 30-day-old (lower panels) Wt and *rima-2* plants. Scale bar: 1 mm. (C) Expression of the *ProSTM:GUS* shoot meristem marker in 5-day-old seedlings. Scale bar: 100 μm. (D) Images of the primary stem from a *rima-2* plant. All *rima-2* plants developed fasciated meristems with split primary SAMs. Scale bar: 1 mm. Upper inset shows enlarged image of a duplicated flower and lower inset shows a duplicated silique from a *rima-2* plant (on average there were more than one duplicated flower per plant, n=150 plants). (E) Images of the cotyledon epidermis from 6-day-old seedlings. The *rima-2* mutant retains small protoderm-like cells that express the *ProTMM: TMM-GFP* marker. Scale bar: 25 μm. Inset shows cluster of stomata in cotyledons of 10-day-old *rima-2* plants. Scale bar: 12.5 μm. (F) Images of cleared root apical meristems from 5-day-old Wt and *rima-2* plants. Cell tracings of the files marked with the brackets are shown to highlight the ectopic periclinal divisions in the mutant. Arrow: quiescent center. Scale bar: 25 μm. (G) Expression of the *J2341* columella initials marker in 5-day-old seedlings. Arrow: quiescent center. Scale bar: 20 μm. (H) Northern analysis of RNA samples from inflorescences of Wt and *rima-2* plants. The arrowhead marks the full-length *RIMA* transcript and the asterisk marks a truncated transcript that accumulates in the mutant. rRNA is shown as a loading control. (I) Images of 14-day-old (upper panels) and 60-day-old (lower panels) *rima-2* and *rima-1/rima-2* plants. Scale bar: 1 mm. (J) Aerial view of a 12-day-old Wt plant, a *rima-2* mutant, and two representative lines of *rima-1* transformed with *ProRIMA:RIMA-GFP* or *Pro35S:RIMA-GFP*. In the lower panel, the expression level of the transgenes in each of the genotypes from the top panel was determined by immunoblot with anti-GFP antibodies. (K) Two examples of twin globular embryos formed in seeds from a representative line of *rima-1* transformed with *Pro35S:RIMA-GFP* (5% of seeds had twin embryos, n=162). Scale bar: 25 μm.

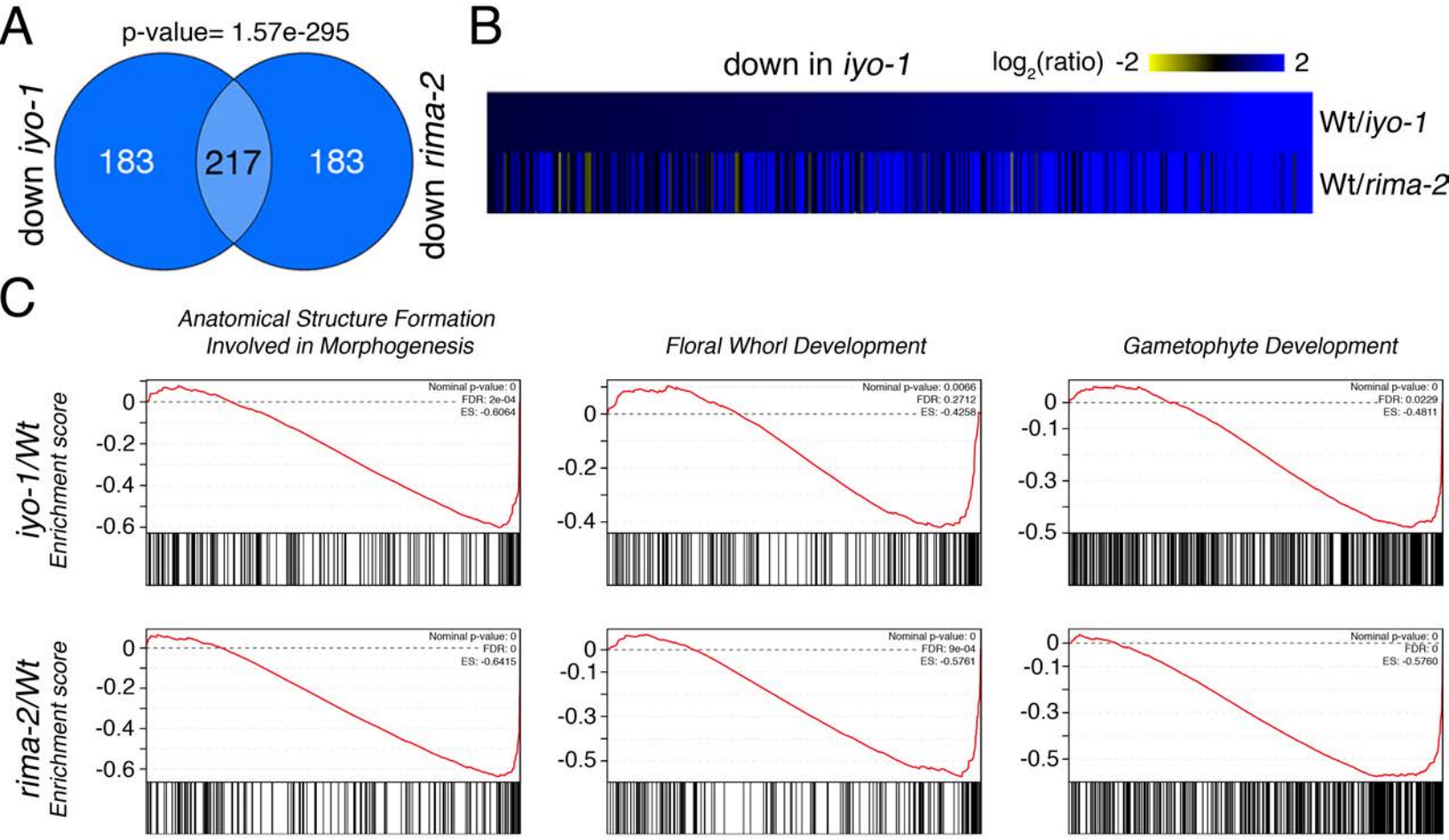

Figure 4. *IYO* and *RIMA* activate transcription of common developmental programs. (A) Venn diagram analysis of the overlap between the sets of 400 genes most down-regulated in *iyo-1*/Wt (down *iyo-1*) and *rima-2*/Wt (down *rima-2*) inflorescences. The p-value (Hypergeometric test) for the observed level of overlap is shown above the graphs. (B) Graphical display of microarray expression data (log_2 of the expression ratio) in Wt versus *iyo-1* (Wt/*iyo-1*) and Wt versus *rima-2* (*Wt/rima-2*) of the 400 genes most highly down-regulated in *iyo-1* inflorescences (Sanmartin et al., 2011). (C) GSEA analysis of gene sets significantly down-regulated in *iyo-1*/Wt and *rima-2*/Wt inflorescence apices.

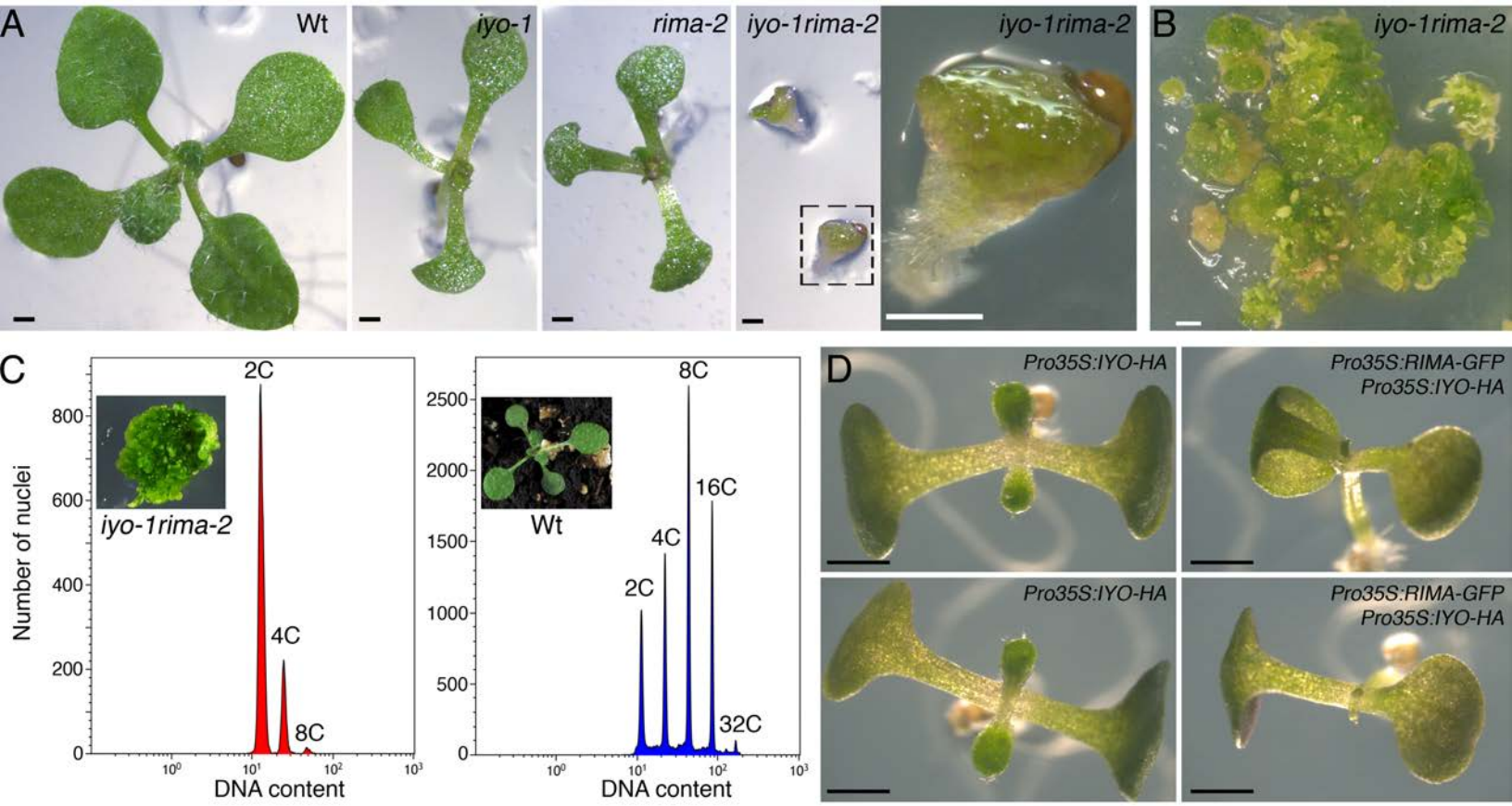

Figure 5. *IYO* and *RIMA* interact genetically to activate differentiation. (A) Images of 10-day-old plants (genotypes as indicated in the panels). A magnification of the framed *iyo-1 rima-2* seedling is shown on the right panel. Scale bar: 0.5 mm. (B) 80-day-old *iyo-1 rima-2* plant. Scale bar: 2 mm. (C) Flow cytometry analysis of nuclear DNA content in 45-day-old *iyo-1 rima-2* mutants. The DNA content of the first pair of leaves from 18-day-old wild-type plants is shown for comparison. (D) Images from 11-day-old plants (genotypes as indicated in the panels). Scale bar: 1mm.

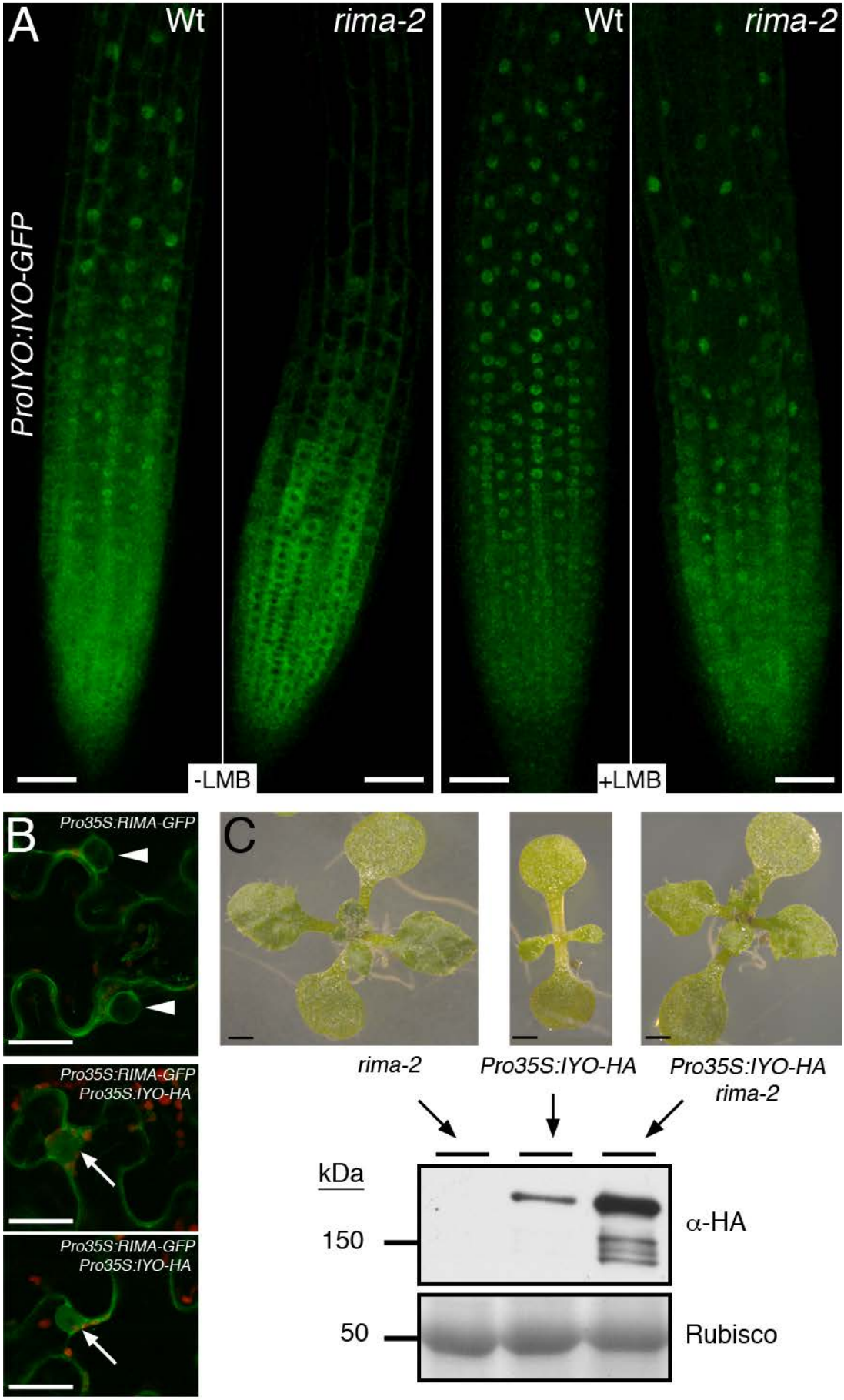

Figure 6. RIMA is required for IYO nuclear accumulation and for its pro-differentiation activity. (A) Confocal images of roots from a *ProIYO:IYO-GFP* line in a Wt background or introgressed into a *rima-2* mutant background (*rima-2*) mock treated (-LMB) or incubated with 0.9 μM LMB for 2.5 hours (+LMB). Scale bar: 50 μm. (B) Confocal images of *N. benthamiana* leaf epidermal cells transiently transformed with *Pro35S:RIMA-GFP* alone or together with *Pro35S:IYO-HA*. Arrowheads mark nuclei with low internal fluorescence and arrows nuclei with high internal fluorescence. Scale bar: 25 μm. (C) Images of 14-day-old *rima-2*, *Pro35S:IYO-HA*, and *Pro35S:IYO-HA rima-2* plants. Scale bar: 1 mm. In the lower panel, IYO-HA expression in plants from the genotypes shown was determined by immunoblotting with anti-HA antibodies.

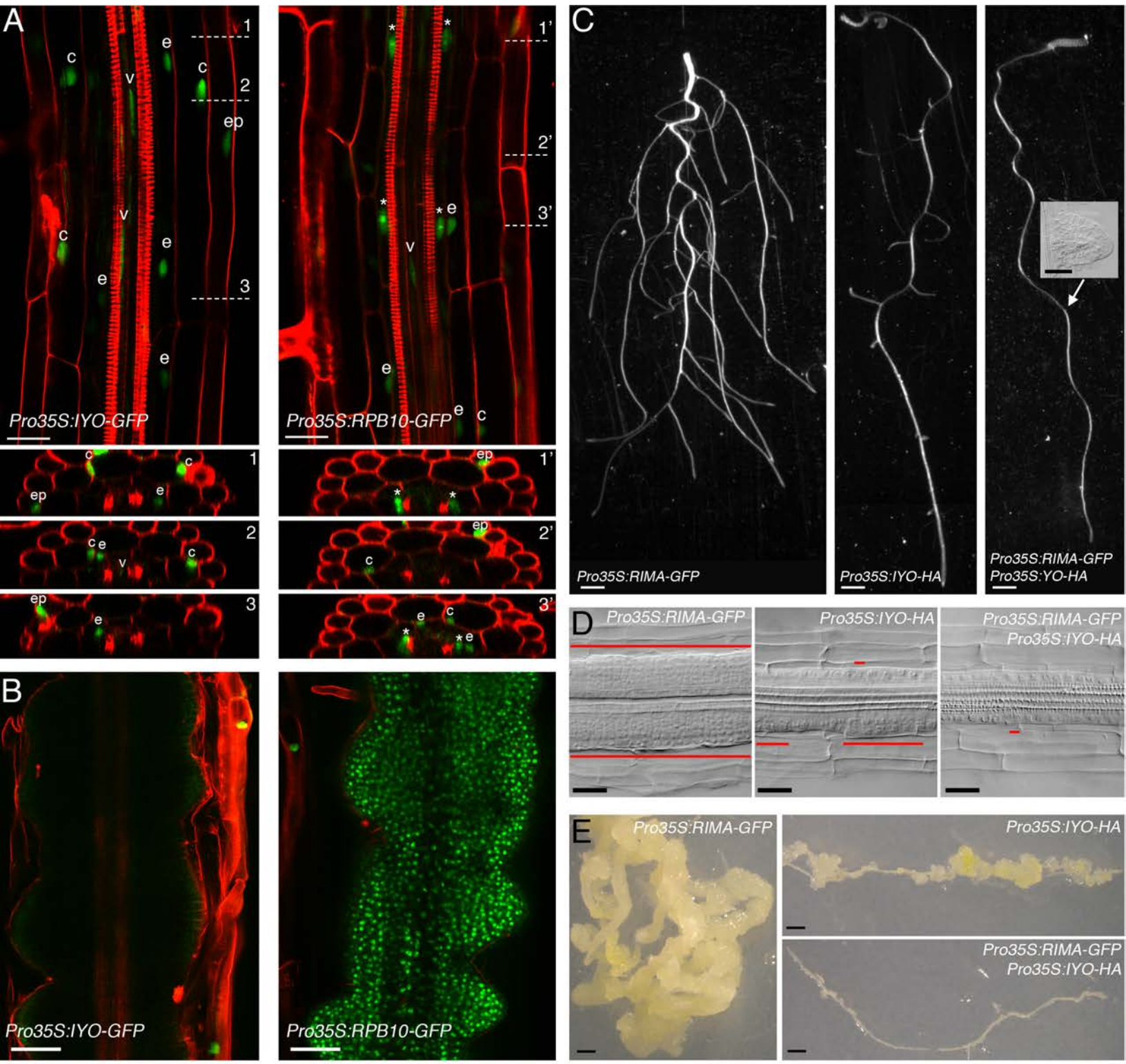

Figure 7. Overexpression of *IYO* and *RIMA* blocks callus formation (A-B) Confocal images of *Pro35S:IYO-GFP* and *Pro35S:RPB10-GFP* plants. Note that root development and RAM size in the transgenic *Pro35S:IYO-GFP* line was indistinguishable from *Pro35S:RPB10-GFP* and Wt plants. (A) Single confocal longitudinal sections at the equatorial plane containing the two xylem poles of roots from 5-day-old plants (top panels). Orthogonal views of the roots reconstructed from serial sections are shown in the bottom panels. The positions of the orthogonal sections are marked on the top panels. Asterisks mark GFP positive nuclei from the xylem pole pericycle. Nuclei from other cell layers are identified by the letters. ep: epidermis; c: cortex; e: endodermis; v: vasculature; Scale bar: 25 μm. (B) Confocal images from roots of 6-day-old plants treated for 3 days in liquid MS medium containing 300 ng/ml of 2,4D. Scale bar: 50 μm. (C-E) Images from *Pro35S:RIMA-GFP, Pro35S:IYO-HA* and *Pro35S:RIMA-GFP Pro35S:IYO-HA* double transgenic plants. Note that Wt plants were indistinguishable from *Pro35S:RIMA-GFP* plants and are not shown. (C) Roots from 14-day-old plants. Scale bar: 1 mm. Inset shows a Nomarski image of the only root primordia emerged in a *Pro35S:RIMA-GFP Pro35S:IYO-HA* plant. Scale bar: 50 μm (D) Nomarski images of sections from the mature zone of the root from 24-day-old plants cultured for 5 days in callus-inducing medium. Red bars mark pericycle domains where periclinal divisions have taken place. Scale bar: 25 μm. (E) Images of sections from the mature zone of the root from 24-day-old plants cultured for 41 days in callus-inducing medium. Scale bar: 1 mm.

Parsed Citations

Atta, R., Laurens, L., Boucheron-Dubuisson, E., Guivarc'h, A., Carnero, E., Giraudat-Pautot, V., Rech, P., and Chriqui, D. (2009). Pluripotency of Arabidopsis xylem pericycle underlies shoot regeneration from root and hypocotyl explants grown in vitro. Plant J 57, 626-644.

Pubmed: Author and Title
CrossRef: Author and Title
Google Scholar: Author Only Title Only Author and Title

Beeckman, T., Burssens, S., and Inze, D. (2001). The peri-cell-cycle in Arabidopsis. J Exp Bot 52, 403-411.

Pubmed: Author and Title
CrossRef: Author and Title
Google Scholar: Author Only Title Only Author and Title

Benfey, P.N. (2016). Defining the Path from Stem Cells to Differentiated Tissue. Curr Top Dev Biol 116, 35-43.

Pubmed: Author and Title
CrossRef: Author and Title
Google Scholar: Author Only Title Only Author and Title

Boulon, S., Pradet-Balade, B., Verheggen, C., Molle, D., Boireau, S., Georgieva, M., Azzag, K., Robert, M.C., Ahmad, Y., Neel, H., Lamond, A.I., and Bertrand, E. (2010). HSP90 and its R2TP/Prefoldin-like cochaperone are involved in the cytoplasmic assembly of RNA polymerase II. Mol Cell 39, 912-924.

Pubmed: Author and Title
CrossRef: Author and Title
Google Scholar: Author Only Title Only Author and Title

Brookes, E., de Santiago, I., Hebenstreit, D., Morris, K.J., Carroll, T., Xie, S.Q., Stock, J.K., Heidemann, M., Eick, D., Nozaki, N., Kimura, H., Ragoussis, J., Teichmann, S.A., and Pombo, A. (2012). Polycomb associates genome-wide with a specific RNA polymerase II variant, and regulates metabolic genes in ESCs. Cell Stem Cell 10, 157-170.

Pubmed: Author and Title
CrossRef: Author and Title
Google Scholar: Author Only Title Only Author and Title

Calera, M.R., Zamora-Ramos, C., Araiza-Villanueva, M.G., Moreno-Aguilar, C.A., Pena-Gomez, S.G., Castellanos-Teran, F., Robledo-Rivera, A.Y., and Sanchez-Olea, R. (2011). Parcs/Gpn3 is required for the nuclear accumulation of RNA polymerase II. Biochim Biophys Acta 1813, 1708-1716.

Pubmed: Author and Title
CrossRef: Author and Title
Google Scholar: Author Only Title Only Author and Title

Carre, C., and Shiekhattar, R. (2011). Human GTPases associate with RNA polymerase II to mediate its nuclear import. Mol Cell Biol 31, 3953-3962.

Pubmed: Author and Title
CrossRef: Author and Title
Google Scholar: Author Only Title Only Author and Title

Che, P., Lall, S., and Howell, S.H. (2007). Developmental steps in acquiring competence for shoot development in Arabidopsis tissue culture. Planta 226, 1183-1194.

Pubmed: Author and Title
CrossRef: Author and Title
Google Scholar: Author Only Title Only Author and Title

Cheng, Y., Cao, L., Wang, S., Li, Y., Shi, X., Liu, H., Li, L., Zhang, Z., Fowke, L.C., Wang, H., and Zhou, Y. (2015). Downregulation of multiple CDK inhibitor ICK/KRP genes upregulates the E2F pathway and increases cell proliferation, and organ and seed sizes in Arabidopsis. Plant J 75, 642-655.

Pubmed: Author and Title
CrossRef: Author and Title
Google Scholar: Author Only Title Only Author and Title

Chupeau, M.C., Granier, F., Pichon, O., Renou, J.P., Gaudin, V., and Chupeau, Y. (2013). Characterization of the early events leading to totipotency in an Arabidopsis protoplast liquid culture by temporal transcript profiling. Plant Cell 25, 2444-2463.

Pubmed: Author and Title
CrossRef: Author and Title
Google Scholar: Author Only Title Only Author and Title

DiDonato, R.J., Arbuckle, E., Buker, S., Sheets, J., Tobar, J., Totong, R., Grisafi, P., Fink, G.R., and Celenza, J.L. (2004). Arabidopsis ALF4 encodes a nuclear-localized protein required for lateral root formation. Plant J 37, 340-353.

Pubmed: Author and Title
CrossRef: Author and Title
Google Scholar: Author Only Title Only Author and Title

Dubrovsky, J.G., Doerner, P.W., Colon-Carmona, A., and Rost, T.L. (2000). Pericycle cell proliferation and lateral root initiation in Arabidopsis. Plant Physiol 124, 1648-1657.

Pubmed: Author and Title
CrossRef: Author and Title
Google Scholar: Author Only Title Only Author and Title

Egloff, S., Zaborowska, J., Laitem, C., Kiss, T., and Murphy, S. (2012). Ser7 phosphorylation of the CTD recruits the RPAP2 Ser5 phosphatase to snRNA genes. Mol Cell 45, 111-122.

Pubmed: Author and Title
CrossRef: Author and Title
Google Scholar: Author Only Title Only Author and Title

Fan, M., Xu, C., Xu, K., and Hu, Y. (2012). LATERAL ORGAN BOUNDARIES DOMAIN transcription factors direct callus formation in Arabidopsis regeneration. Cell Res 22, 1169-1180.
Pubmed: Author and Title
CrossRef: Author and Title
Google Scholar: Author Only Title Only Author and Title

Forget, D., Lacombe, A.A., Cloutier, P., Lavallee-Adam, M., Blanchette, M., and Coulombe, B. (2013). Nuclear import of RNA polymerase II is coupled with nucleocytoplasmic shuttling of the RNA polymerase II-associated protein 2. Nucleic Acids Res 41, 6881-6891.
Pubmed: Author and Title
CrossRef: Author and Title
Google Scholar: Author Only Title Only Author and Title

Forget, D., Lacombe, A.A., Cloutier, P., Al-Khoury, R., Bouchard, A., Lavallee-Adam, M., Faubert, D., Jeronimo, C., Blanchette, M., and Coulombe, B. (2010). The protein interaction network of the human transcription machinery reveals a role for the conserved GTPase RPAP4/GPN1 and microtubule assembly in nuclear import and biogenesis of RNA polymerase II. Mol Cell Proteomics 9, 2827-2839.
Pubmed: Author and Title
CrossRef: Author and Title
Google Scholar: Author Only Title Only Author and Title

Fukaki, H., Okushima, Y., and Tasaka, M. (2007). Auxin-mediated lateral root formation in higher plants. Int Rev Cytol 256, 111-137.
Pubmed: Author and Title
CrossRef: Author and Title
Google Scholar: Author Only Title Only Author and Title

Fukaki, H., Tameda, S., Masuda, H., and Tasaka, M. (2002). Lateral root formation is blocked by a gain-of-function mutation in the SOLITARY-ROOT/IAA14 gene of Arabidopsis. Plant J 29, 153-168.
Pubmed: Author and Title
CrossRef: Author and Title
Google Scholar: Author Only Title Only Author and Title

Gaillochet, C., and Lohmann, J.U. (2015). The never-ending story: from pluripotency to plant developmental plasticity. Development 142, 2237-2249.
Pubmed: Author and Title
CrossRef: Author and Title
Google Scholar: Author Only Title Only Author and Title

Galbraith, D.W., Harkins, K.R., Maddox, J.M., Ayres, N.M., Sharma, D.P., and Firoozabady, E. (1983). Rapid flow cytometric analysis of the cell cycle in intact plant tissues. Science 220, 1049-1051.
Pubmed: Author and Title
CrossRef: Author and Title
Google Scholar: Author Only Title Only Author and Title

Giaever, G., Chu, A.M., Ni, L., Connelly, C., Riles, L., Veronneau, S., Dow, S., Lucau-Danila, A., Anderson, K., Andre, B., Arkin, A.P., Astromoff, A., El-Bakkoury, M., Bangham, R., Benito, R., Brachat, S., Campanaro, S., Curtiss, M., Davis, K., Deutschbauer, A., Entian, K.D., Flaherty, P., Foury, F., Garfinkel, D.J., Gerstein, M., Gotte, D., Guldener, U., Hegemann, J.H., Hempel, S., Herman, Z., Jaramillo, D.F., Kelly, D.E., Kelly, S.L., Kotter, P., LaBonte, D., Lamb, D.C., Lan, N., Liang, H., Liao, H., Liu, L., Luo, C., Lussier, M., Mao, R., Menard, P., Ooi, S.L., Revuelta, J.L., Roberts, C.J., Rose, M., Ross-Macdonald, P., Scherens, B., Schimmack, G., Shafer, B., Shoemaker, D.D., Sookhai-Mahadeo, S., Storms, R.K., Strathern, J.N., Valle, G., Voet, M., Volckaert, G., Wang, C.Y., Ward, T.R., Wilhelmy, J., Winzeler, E.A., Yang, Y., Yen, G., Youngman, E., Yu, K., Bussey, H., Boeke, J.D., Snyder, M., Philippsen, P., Davis, R.W., and Johnston, M. (2002). Functional profiling of the Saccharomyces cerevisiae genome. Nature 418, 387-391.
Pubmed: Author and Title
CrossRef: Author and Title
Google Scholar: Author Only Title Only Author and Title

Gibney, P.A., Fries, T., Bailer, S.M., and Morano, K.A. (2008). Rtr1 is the Saccharomyces cerevisiae homolog of a novel family of RNA polymerase II-binding proteins. Eukaryot Cell 7, 938-948.
Pubmed: Author and Title
CrossRef: Author and Title
Google Scholar: Author Only Title Only Author and Title

Gomez-Navarro, N., and Estruch, F. (2015). Different pathways for the nuclear import of yeast RNA polymerase II. Biochim Biophys Acta 1849, 1354-1362.
Pubmed: Author and Title
CrossRef: Author and Title
Google Scholar: Author Only Title Only Author and Title

Guenther, M.G., Levine, S.S., Boyer, L.A., Jaenisch, R., and Young, R.A. (2007). A chromatin landmark and transcription initiation at most promoters in human cells. Cell 130, 77-88.
Pubmed: Author and Title
CrossRef: Author and Title
Google Scholar: Author Only Title Only Author and Title

Haasen, D., Kohler, C., Neuhaus, G., and Merkle, T. (1999). Nuclear export of proteins in plants: AtXPO1 is the export receptor for leucine-rich nuclear export signals in Arabidopsis thaliana. Plant J 20, 695-705.

Pubmed: Author and Title
CrossRef: Author and Title
Google Scholar: Author Only Title Only Author and Title

Hsu, P.L., Yang, F., Smith-Kinnaman, W., Yang, W., Song, J.E., Mosley, A.L., and Varani, G. (2014). Rtr1 Is a Dual Specificity Phosphatase That Dephosphorylates Tyr1 and Ser5 on the RNA Polymerase II CTD. J Mol Biol 426, 2970-2981.
Pubmed: Author and Title
CrossRef: Author and Title
Google Scholar: Author Only Title Only Author and Title

Hunter, G.O., Fox, M.J., Smith-Kinnaman, W.R., Gogol, M., Fleharty, B., and Mosley, A.L. (2016). Phosphatase Rtr1 Regulates Global Levels of Serine 5 RNA Polymerase II C-Terminal Domain Phosphorylation and Cotranscriptional Histone Methylation. Mol Cell Biol 36, 2236-2245.
Pubmed: Author and Title
CrossRef: Author and Title
Google Scholar: Author Only Title Only Author and Title

Ikeuchi, M., Sugimoto, K., and Iwase, A. (2013). Plant callus: mechanisms of induction and repression. Plant Cell 25, 3159-3173.
Pubmed: Author and Title
CrossRef: Author and Title
Google Scholar: Author Only Title Only Author and Title

Ikeuchi, M., Iwase, A., Rymen, B., Harashima, H., Shibata, M., Ohnuma, M., Breuer, C., Morao, A.K., de Lucas, M., De Veylder, L., Goodrich, J., Brady, S.M., Roudier, F., and Sugimoto, K. (2015). PRC2 represses dedifferentiation of mature somatic cells in Arabidopsis. Nat Plants 1, 15089.
Pubmed: Author and Title
CrossRef: Author and Title
Google Scholar: Author Only Title Only Author and Title

Irani, S., Yogesha, S.D., Mayfield, J., Zhang, M., Zhang, Y., Matthews, W.L., Nie, G., Prescott, N.A., and Zhang, Y.J. (2016). Structure of Saccharomyces cerevisiae Rtr1 reveals an active site for an atypical phosphatase. Sci Signal 9, ra24.
Pubmed: Author and Title
CrossRef: Author and Title
Google Scholar: Author Only Title Only Author and Title

Iwase, A., Ohme-Takagi, M., and Sugimoto, K. (2011a). WIND1: a key molecular switch for plant cell dedifferentiation. Plant Signal Behav 6, 1943-1945.
Pubmed: Author and Title
CrossRef: Author and Title
Google Scholar: Author Only Title Only Author and Title

Iwase, A., Mitsuda, N., Koyama, T., Hiratsu, K., Kojima, M., Arai, T., Inoue, Y., Seki, M., Sakakibara, H., Sugimoto, K., and Ohme-Takagi, M. (2011b). The AP2/ERF transcription factor WIND1 controls cell dedifferentiation in Arabidopsis. Curr Biol 21, 508-514.
Pubmed: Author and Title
CrossRef: Author and Title
Google Scholar: Author Only Title Only Author and Title

Jen, C.H., Manfield, I.W., Michalopoulos, I., Pinney, J.W., Willats, W.G., Gilmartin, P.M., and Westhead, D.R. (2006). The Arabidopsis co-expression tool (ACT): a WWW-based tool and database for microarray-based gene expression analysis. Plant J 46, 336-348.
Pubmed: Author and Title
CrossRef: Author and Title
Google Scholar: Author Only Title Only Author and Title

Jeronimo, C., Forget, D., Bouchard, A., Li, Q., Chua, G., Poitras, C., Therien, C., Bergeron, D., Bourassa, S., Greenblatt, J., Chabot, B., Poirier, G.G., Hughes, T.R., Blanchette, M., Price, D.H., and Coulombe, B. (2007). Systematic analysis of the protein interaction network for the human transcription machinery reveals the identity of the 7SK capping enzyme. Mol Cell 27, 262-274.
Pubmed: Author and Title
CrossRef: Author and Title
Google Scholar: Author Only Title Only Author and Title

Jeronimo, C., Langelier, M.F., Zeghouf, M., Cojocaru, M., Bergeron, D., Baali, D., Forget, D., Mnaimneh, S., Davierwala, A.P., Pootoolal, J., Chandy, M., Canadien, V., Beattie, B.K., Richards, D.P., Workman, J.L., Hughes, T.R., Greenblatt, J., and Coulombe, B. (2004). RPAP1, a novel human RNA polymerase II-associated protein affinity purified with recombinant wild-type and mutated polymerase subunits. Mol Cell Biol 24, 7043-7058.
Pubmed: Author and Title
CrossRef: Author and Title
Google Scholar: Author Only Title Only Author and Title

Kaufmann, K., Pajoro, A., and Angenent, G.C. (2010). Regulation of transcription in plants: mechanisms controlling developmental switches. Nat Rev Genet 11, 830-842.
Pubmed: Author and Title
CrossRef: Author and Title
Google Scholar: Author Only Title Only Author and Title

Lahmy, S., Guilleminot, J., Schmit, A.C., Pelletier, G., Chaboute, M.E., and Devic, M. (2007). QQT proteins colocalize with microtubules and are essential for early embryo development in Arabidopsis. Plant J 50, 615-626.
Pubmed: Author and Title
CrossRef: Author and Title
Google Scholar: Author Only Title Only Author and Title

Lee, H.W., Kim, N.Y., Lee, D.J., and Kim, J. (2009). LBD18/ASL20 regulates lateral root formation in combination with LBD16/ASL18 downstream of ARF7 and ARF19 in Arabidopsis. Plant Physiol 151, 1377-1389.
Pubmed: Author and Title
CrossRef: Author and Title
Google Scholar: Author Only Title Only Author and Title

Lee, T.I., and Young, R.A. (2013). Transcriptional regulation and its misregulation in disease. Cell 152, 1237-1251.
Pubmed: Author and Title
CrossRef: Author and Title
Google Scholar: Author Only Title Only Author and Title

Liu, J., Sheng, L., Xu, Y., Li, J., Yang, Z., Huang, H., and Xu, L. (2014). WOX11 and 12 are involved in the first-step cell fate transition during de novo root organogenesis in Arabidopsis. Plant Cell 26, 1081-1093.
Pubmed: Author and Title
CrossRef: Author and Title
Google Scholar: Author Only Title Only Author and Title

Minaker, S.W., Filiatrault, M.C., Ben-Aroya, S., Hieter, P., and Stirling, P.C. (2013). Biogenesis of RNA polymerases II and III requires the conserved GPN small GTPases in Saccharomyces cerevisiae. Genetics 193, 853-864.
Pubmed: Author and Title
CrossRef: Author and Title
Google Scholar: Author Only Title Only Author and Title

Mosley, A.L., Pattenden, S.G., Carey, M., Venkatesh, S., Gilmore, J.M., Florens, L., Workman, J.L., and Washburn, M.P. (2009). Rtr1 is a CTD phosphatase that regulates RNA polymerase II during the transition from serine 5 to serine 2 phosphorylation. Mol Cell 34, 168-178.
Pubmed: Author and Title
CrossRef: Author and Title
Google Scholar: Author Only Title Only Author and Title

Ni, Z., Xu, C., Guo, X., Hunter, G.O., Kuznetsova, O.V., Tempel, W., Marcon, E., Zhong, G., Guo, H., Kuo, W.H., Li, J., Young, P., Olsen, J.B., Wan, C., Loppnau, P., El Bakkouri, M., Senisterra, G.A., He, H., Huang, H., Sidhu, S.S., Emili, A., Murphy, S., Mosley, A.L., Arrowsmith, C.H., Min, J., and Greenblatt, J.F. (2014). RPRD1A and RPRD1B are human RNA polymerase II C-terminal domain scaffolds for Ser5 dephosphorylation. Nat Struct Mol Biol 21, 686-695.
Pubmed: Author and Title
CrossRef: Author and Title
Google Scholar: Author Only Title Only Author and Title

Niesser, J., Wagner, F.R., Kostrewa, D., Muhlbacher, W., and Cramer, P. (2016). Structure of GPN-Loop GTPase Npa3 and Implications for RNA Polymerase II Assembly. Mol Cell Biol 36, 820-831.
Pubmed: Author and Title
CrossRef: Author and Title
Google Scholar: Author Only Title Only Author and Title

Okushima, Y., Fukaki, H., Onoda, M., Theologis, A., and Tasaka, M. (2007). ARF7 and ARF19 regulate lateral root formation via direct activation of LBD/ASL genes in Arabidopsis. Plant Cell 19, 118-130.
Pubmed: Author and Title
CrossRef: Author and Title
Google Scholar: Author Only Title Only Author and Title

Perianez-Rodriguez, J., Manzano, C., and Moreno-Risueno, M.A. (2014). Post-embryonic organogenesis and plant regeneration from tissues: two sides of the same coin? Front Plant Sci 5, 219.
Pubmed: Author and Title
CrossRef: Author and Title
Google Scholar: Author Only Title Only Author and Title

Pijnappel, W.W., Esch, D., Baltissen, M.P., Wu, G., Mischerikow, N., Bergsma, A.J., van der Wal, E., Han, D.W., Bruch, H., Moritz, S., Lijnzaad, P., Altelaar, A.F., Sameith, K., Zaehres, H., Heck, A.J., Holstege, F.C., Scholer, H.R., and Timmers, H.T. (2013). A central role for TFIID in the pluripotent transcription circuitry. Nature 495, 516-519.
Pubmed: Author and Title
CrossRef: Author and Title
Google Scholar: Author Only Title Only Author and Title

Sablowski, R. (2011). Plant stem cell niches: from signalling to execution. Curr Opin Plant Biol 14, 4-9.
Pubmed: Author and Title
CrossRef: Author and Title
Google Scholar: Author Only Title Only Author and Title

Sablowski, R. (2015). Control of patterning, growth, and differentiation by floral organ identity genes. J Exp Bot 66, 1065-1073.
Pubmed: Author and Title
CrossRef: Author and Title
Google Scholar: Author Only Title Only Author and Title

Sanchez Alvarado, A., and Yamanaka, S. (2014). Rethinking differentiation: stem cells, regeneration, and plasticity. Cell 157, 110-119.
Pubmed: Author and Title
CrossRef: Author and Title
Google Scholar: Author Only Title Only Author and Title

Sanmartin, M., Sauer, M., Munoz, A., and Rojo, E. (2012). MINIYO and transcriptional elongation: lifting the roadblock to

differentiation. Transcription 3, 25-28.
Pubmed: Author and Title
CrossRef: Author and Title
Google Scholar: Author Only Title Only Author and Title

Sanmartin, M., Sauer, M., Munoz, A., Zouhar, J., Ordonez, A., van de Ven, W.T., Caro, E., de la Paz Sanchez, M., Raikhel, N.V., Gutierrez, C., Sanchez-Serrano, J.J., and Rojo, E. (2011). A molecular switch for initiating cell differentiation in Arabidopsis. Curr Biol 21, 999-1008.
Pubmed: Author and Title
CrossRef: Author and Title
Google Scholar: Author Only Title Only Author and Title

Sanz, L., Dewitte, W., Forzani, C., Patell, F., Nieuwland, J., Wen, B., Quelhas, P., De Jager, S., Titmus, C., Campilho, A., Ren, H., Estelle, M., Wang, H., and Murray, J.A. (2011). The Arabidopsis D-type cyclin CYCD2;1 and the inhibitor ICK2/KRP2 modulate auxin-induced lateral root formation. Plant Cell 23, 641-660.
Pubmed: Author and Title
CrossRef: Author and Title
Google Scholar: Author Only Title Only Author and Title

Scheres, B. (2007). Stem-cell niches: nursery rhymes across kingdoms. Nat Rev Mol Cell Biol 8, 345-354.
Pubmed: Author and Title
CrossRef: Author and Title
Google Scholar: Author Only Title Only Author and Title

Sena, G., Wang, X., Liu, H.Y., Hofhuis, H., and Birnbaum, K.D. (2009). Organ regeneration does not require a functional stem cell niche in plants. Nature 457, 1150-1153.
Pubmed: Author and Title
CrossRef: Author and Title
Google Scholar: Author Only Title Only Author and Title

Shang, B., Xu, C., Zhang, X., Cao, H., Xin, W., and Hu, Y. (2016). Very-long-chain fatty acids restrict regeneration capacity by confining pericycle competence for callus formation in Arabidopsis. Proc Natl Acad Sci U S A 113, 5101-5106.
Pubmed: Author and Title
CrossRef: Author and Title
Google Scholar: Author Only Title Only Author and Title

Staresincic, L., Walker, J., Dirac-Svejstrup, A.B., Mitter, R., and Svejstrup, J.Q. (2011). GTP-dependent binding and nuclear transport of RNA polymerase II by Npa3 protein. J Biol Chem 286, 35553-35561.
Pubmed: Author and Title
CrossRef: Author and Title
Google Scholar: Author Only Title Only Author and Title

Stock, J.K., Giadrossi, S., Casanova, M., Brookes, E., Vidal, M., Koseki, H., Brockdorff, N., Fisher, A.G., and Pombo, A. (2007). Ring1-mediated ubiquitination of H2A restrains poised RNA polymerase II at bivalent genes in mouse ES cells. Nat Cell Biol 9, 1428-1435.
Pubmed: Author and Title
CrossRef: Author and Title
Google Scholar: Author Only Title Only Author and Title

Su, Y.H., and Zhang, X.S. (2014). The hormonal control of regeneration in plants. Curr Top Dev Biol 108, 35-69.
Pubmed: Author and Title
CrossRef: Author and Title
Google Scholar: Author Only Title Only Author and Title

Sugimoto, K., Jiao, Y., and Meyerowitz, E.M. (2010). Arabidopsis regeneration from multiple tissues occurs via a root development pathway. Dev Cell 18, 463-471.
Pubmed: Author and Title
CrossRef: Author and Title
Google Scholar: Author Only Title Only Author and Title

Sugimoto, K., Gordon, S.P., and Meyerowitz, E.M. (2011). Regeneration in plants and animals: dedifferentiation, transdifferentiation, or just differentiation? Trends Cell Biol 21, 212-218.
Pubmed: Author and Title
CrossRef: Author and Title
Google Scholar: Author Only Title Only Author and Title

Sugiyama, M. (2015). Historical review of research on plant cell dedifferentiation. J Plant Res 128, 349-359.
Pubmed: Author and Title
CrossRef: Author and Title
Google Scholar: Author Only Title Only Author and Title

Van Lijsebettens, M., and Grasser, K.D. (2014). Transcript elongation factors: shaping transcriptomes after transcript initiation. Trends Plant Sci 19, 717-726.
Pubmed: Author and Title
CrossRef: Author and Title
Google Scholar: Author Only Title Only Author and Title

Wani, S., Hirose, Y., and Ohkuma, Y. (2014). Human RNA polymerase II-associated protein 2 (RPAP2) interacts directly with the RNA polymerase II subunit Rpb6 and participates in pre-mRNA 3'-end formation. Drug Discov Ther 8, 255-261.
Pubmed: Author and Title
CrossRef: Author and Title
Google Scholar: Author Only Title Only Author and Title

Wolters, H., and Jurgens, G. (2009). Survival of the flexible: hormonal growth control and adaptation in plant development. Nat Rev Genet 10, 305-317.
Pubmed: Author and Title
CrossRef: Author and Title
Google Scholar: Author Only Title Only Author and Title

Xiang, K., Manley, J.L., and Tong, L. (2012). The yeast regulator of transcription protein Rtr1 lacks an active site and phosphatase activity. Nat Commun 3, 946.
Pubmed: Author and Title
CrossRef: Author and Title
Google Scholar: Author Only Title Only Author and Title

Young, R.A. (2011). Control of the embryonic stem cell state. Cell 144, 940-954.
Pubmed: Author and Title
CrossRef: Author and Title
Google Scholar: Author Only Title Only Author and Title

Zhang, T.Q., Lian, H., Tang, H., Dolezal, K., Zhou, C.M., Yu, S., Chen, J.H., Chen, Q., Liu, H., Ljung, K., and Wang, J.W. (2015). An intrinsic microRNA timer regulates progressive decline in shoot regenerative capacity in plants. Plant Cell 27, 349-360.
Pubmed: Author and Title
CrossRef: Author and Title
Google Scholar: Author Only Title Only Author and Title

RIMA-dependent nuclear accumulation of IYO triggers auxin-irreversible cell differentiation in Arabidopsis

Alfonso Muñoz, Silvina Mangano, Mary Paz González-García, Ramón Contreras, Michael B Sauer, Bert De Rybel, Dolf Weijers, José J. Sánchez-Serrano, Maite Sanmartín and Enrique Rojo

Plant Cell; originally published online February 21, 2017;
DOI 10.1105/tpc.16.00791